

# Biomass burning emissions of trace gases and particles in marine air at Cape Grim, Tasmania.

S.J. Lawson<sup>1</sup>, M.D. Keywood<sup>1</sup>, I.E. Galbally<sup>1</sup>, J.L. Gras<sup>1</sup>, J.M. Caine<sup>1,2</sup>, M.E. Cope<sup>1</sup>, P.B. Krummel<sup>1</sup>, P.J. Fraser<sup>1</sup>, L.P. Steele<sup>1</sup>, S.T. Bentley<sup>†</sup>, C.P Meyer<sup>1</sup>, Z. Ristovski<sup>3</sup> and A.H. Goldstein<sup>4</sup>

[1]{Commonwealth Scientific and Industrial Research Organisation, Oceans and Atmosphere, Aspendale, Australia}

[2]{formerly from the Bureau of Meteorology, Smithton, Tasmania, Australia}

[3]{International Laboratory for Air Quality & Health, Queensland University of Technology, Brisbane, Australia}

[4]{Department of Civil and Environmental Engineering, University of California, Berkeley}

Correspondence to: S. J. Lawson (sarah.lawson@csiro.au)

## Abstract

Biomass burning (BB) plumes were measured at the Cape Grim Baseline Air Pollution Station during the 2006 Precursors to Particles campaign, when emissions from a fire on nearby Robbins Island impacted the station. Measurements made included non methane organic compounds (NMOCs) (PTR-MS), particle number size distribution, condensation nuclei (CN) > 3 nm, black carbon (BC) concentration, cloud condensation nuclei (CCN) number, ozone (O<sub>3</sub>), methane (CH<sub>4</sub>), carbon monoxide (CO), hydrogen (H<sub>2</sub>), carbon dioxide (CO<sub>2</sub>), nitrous oxide (N<sub>2</sub>O), halocarbons and meteorology.

During the first plume strike event (BB1), a four hour enhancement of CO (max ~2100 ppb), BC (~1400 ng m<sup>-3</sup>) and particles > 3 nm (~13,000 cm<sup>-3</sup>) with dominant particle mode of 120 nm were observed overnight. A wind direction change lead to a dramatic reduction in BB tracers and a drop in the dominant particle mode to 50 nm. The dominant mode increased in size to 80 nm over 5 hours in calm sunny conditions, accompanied by an increase in ozone. Due to an enhancement in BC but not CO during particle growth, the presence of BB emissions during this period could not be confirmed.

The ability of particles > 80 nm (CN80) to act as CCN at 0.5% supersaturation was investigated. The  $\Delta\text{CCN}/\Delta\text{CN80}$  ratio was lowest during the fresh BB plume (56±8%), higher during the particle growth period (77±4%) and higher still (104±3%) in background

1 marine air. Particle size distributions indicate that changes to particle chemical composition,  
2 rather than particle size, are driving these changes. Hourly average CCN during both BB  
3 events were between 2000-5000 CCN cm<sup>-3</sup>, which were enhanced above typical background  
4 levels by a factor of 6-34, highlighting the dramatic impact BB plumes can have on CCN  
5 number in clean marine regions.

6 During the 29 hours of the second plume strike event (BB2) CO, BC and a range of NMOCs  
7 including acetonitrile and hydrogen cyanide (HCN) were clearly enhanced and some  
8 enhancements in O<sub>3</sub> were observed ( $\Delta O_3/\Delta CO$  0.001-0.074). A shortlived increase in  
9 NMOCs by a factor of 10 corresponded with a large CO enhancement, an increase of the  
10 NMOC/CO emission ratio (ER) by a factor of 2 – 4 and a halving of the BC/CO ratio.  
11 Rainfall on Robbins Island was observed by radar during this period which likely resulted in  
12 a lower fire combustion efficiency, and higher emission of compounds associated with  
13 smouldering. This highlights the importance of relatively minor meteorological events on BB  
14 emission ratios.

15 Emission factors (EF) were derived for a range of trace gases, some never before reported for  
16 Australian fires, (including hydrogen, phenol and toluene) using the carbon mass balance  
17 method. This provides a unique set of EF for Australian coastal heathland fires. Methyl halide  
18 EFs were higher than EF reported from other studies in Australia and the Northern  
19 Hemisphere which is likely due to high halogen content in vegetation on Robbins Island.

20 This work demonstrates the substantial impact that BB plumes can have on the composition  
21 of marine air, and the significant changes that can occur as the plume interacts with  
22 terrestrial, aged urban and marine emission sources.

23

## 24 **1 Introduction**

25 Biomass burning (BB) is the largest global source of primary carbonaceous fine aerosols and  
26 the second largest source of trace gases (Akagi et al., 2011). Species directly emitted from  
27 fires include carbon dioxide (CO<sub>2</sub>), methane (CH<sub>4</sub>), carbon monoxide (CO), nitrogen oxides  
28 (NO<sub>x</sub>), ammonia (NH<sub>3</sub>), non methane organic compounds (NMOCs), carbonyl sulfide (COS),  
29 sulfur dioxide (SO<sub>2</sub>) and elemental and organic carbonaceous and sulphate-containing  
30 particles (Keywood et al., 2011). Secondary species that are formed from BB precursors  
31 include ozone (O<sub>3</sub>), oxygenated NMOCs and inorganic and organic aerosol (OA). The  
32 complex mixture of reactive gases and aerosol that make up BB plumes can act as short lived

1 climate forcers (Keywood et al., 2011). While BB plumes often have the greatest impact on  
2 the atmosphere close to the source of the fire, once injected into the free troposphere plumes  
3 may travel long distances, so that climate and air quality effects may be regional or even  
4 global. A recent modelling study by Lewis et al., (2013) for example highlighted the large  
5 contribution that BB emissions make to the burden of several NMOC in the background  
6 atmosphere, particularly in the Southern Hemisphere.

7 With some studies predicting that future changes to the climate will result in increasing fire  
8 frequency (Keywood et al., 2011), it is essential to understand the composition of fresh  
9 plumes, how they vary temporally and spatially, and the way in which the chemical  
10 composition is transformed with aging. This will provide the process understanding to allow  
11 models to more accurately predict regional air quality impacts and long term climate effects  
12 of BB.

13 Characterising BB plumes is challenging for several reasons, and significant knowledge gaps  
14 still exist. BB plumes contain extremely complex mixtures of trace gases and aerosols, which  
15 vary substantially both spatially and temporally. The initial composition of BB plumes is  
16 dependent on the combustion process and efficiency of combustion, which has a complex  
17 relationship with environmental variables. Combustion efficiency (CE) is a measure of the  
18 fraction of fuel carbon completely oxidised to CO<sub>2</sub>. However it is difficult to measure all the  
19 carbon species required to calculate CE, and so modified combustion efficiency (MCE),  
20 which closely approximates the CE, is often used instead, where  $MCE = \Delta CO_2 /$   
21  $(\Delta CO + \Delta CO_2)$  (Ferek et al., 1998) where  $\Delta$  refers to excess or above-background quantities.  
22 The efficiency of fire combustion depends on fuel size, density and spacing, fuel moisture  
23 content, local meteorology (including temperature, windspeed and precipitation), and terrain  
24 (van Leeuwen and van der Werf, 2011), and MCE can vary substantially spatially and  
25 temporally within one fire. The EF of trace gas and aerosol species are in many cases  
26 strongly tied to the efficiency of combustion. Species such as CO, organic carbon, and  
27 NMOCs tend to be emitted at higher rates in smouldering fires which burn with low MCE  
28 (i.e. have a negative relationship with MCE), while other species such as CO<sub>2</sub> and black  
29 carbon (BC) are emitted at higher rates in flaming fires with higher MCE (e.g. have a positive  
30 relationship with MCE) (Andreae and Merlet, 2001).

31 Once emitted, the composition of BB plumes can change very rapidly, with destruction of  
32 highly reactive species, coagulation of particles, and formation of secondary species such as  
33 O<sub>3</sub>, oxygenated NMOCs and secondary organic and inorganic aerosol occurring on a

1 timescale of minutes to hours (Akagi et al., 2012; Vakkari et al., 2014). Particles typically  
2 become more oxygenated, and particle size often increases as primary particles are coated  
3 either with low-volatility oxidation products of co-emitted organic and inorganic gases, or  
4 with co-emitted semi volatile primary organics (Sahu et al., 2012; Akagi et al., 2012; Vakkari  
5 et al., 2014). Changes that occur in the composition of the plume can be highly variable and  
6 drivers of variability are difficult to quantify. One example is the large variability in the net  
7 OA enhancement in aged BB plumes, with studies reporting both enhancements and  
8 decreases in the OA/CO ratio with plume aging (Yokelson et al., 2009; Hennigan et al., 2011;  
9 Cubison et al., 2011; Akagi et al., 2012; Hecobian et al., 2012).

10 While BB is recognised as a major source of CCN (Andreae et al., 2002), the hygroscopicity  
11 of fresh BB particles varies enormously from weakly to highly hygroscopic and fuel type  
12 appears to be a major driver of the variability (Pratt et al., 2011; Engelhart et al., 2012;  
13 Petters et al., 2009) along with particle morphology (Martin et al., 2013). As particles age, in  
14 addition to becoming larger, they also generally become more hygroscopic and more easily  
15 activated to CCN. However, this is dependent on the initial composition and hygroscopicity  
16 of the particle, as well as the hygroscopicity of the coating material (Martin et al., 2013;  
17 Engelhart et al., 2012). Most studies of CCN in BB plumes to date have been chamber  
18 studies, and there are few ambient studies which have examined the ability of BB particles to  
19 act as CCN in fresh and aged plumes.

20 Ozone is typically destroyed by reaction with nitric oxide (NO) in close proximity to the fire,  
21 however once the plume is diluted, O<sub>3</sub> enhancement is often observed (typically normalised  
22 to CO). In a recent summary of a number of studies, the enhancement of O<sub>3</sub> to CO typically  
23 increases with the age of the plume (Jaffe and Wigder, 2012). However there is significant  
24 variation in O<sub>3</sub> enhancements observed between studies which is thought to be dependent on  
25 several factors such as precursor emissions (resulting from fuel and combustion efficiency),  
26 meteorology, the aerosol affect on plume chemistry and radiation, and photochemical  
27 reactions. Many challenges remain in modelling the transformation processes that occur in  
28 BB plumes, such as O<sub>3</sub> formation and changes to particle properties, in part due to a lack of  
29 high-quality real-time observations (Jaffe and Wigder, 2012; Akagi et al., 2012).

30 In recent years there have been a number of intensive field and laboratory studies which have  
31 characterised both fresh emissions and aged BB emissions. However there are several regions  
32 of the globe where BB emissions, including emission factors (EF), have been sparsely  
33 characterised. For example, EF data has been published for only a few trace gases in the

1 temperate forests of Southern Australian (Volkova et al., 2014; Paton-Walsh et al., 2012;  
2 Paton-Walsh et al., 2005; Paton-Walsh et al., 2014; Paton-Walsh et al., 2008). The lack of  
3 Australian temperate EF was evident in a recent compilation of EF by Akagi et al (2011), in  
4 which all temperate EF reported were from the Northern Hemisphere (NH) from mostly  
5 coniferous forests. Species emitted during combustion can be strongly dependent on  
6 vegetation type (e.g. Simpson et al 2011), and EFs from NH coniferous forests are unlikely to  
7 be representative of for example Australia's temperate dry sclerophyll forests. Using EF from  
8 boreal and tropical forest fires to model BB plumes in temperate regions adds uncertainty to  
9 the model outcomes (Akagi et al., 2011), and more detailed chemical measurements of BB  
10 plumes in the Southern Hemisphere temperate regions are needed.

11 An increasingly wide range of sophisticated instruments are being used to measure the trace  
12 gas and aerosol composition and microphysical properties in BB plumes. This has led to a  
13 higher proportion of NMOC being quantified than ever. Despite this, there is significant  
14 evidence that a large proportion of NMOCs in BB plumes are still not being identified. A  
15 compilation of NMOC measurements from 71 laboratory fires using a range of techniques,  
16 found that the mass of unidentified NMOC was significant (up to 50%) (Yokelson et al.,  
17 2013), though recent work using high-resolution proton transfer reaction – time of flight –  
18 mass spectrometry (PTR-TOF-MS) has allowed at least tentative identification of up to 93%  
19 of NMOC (Stockwell et al., 2015). Flow reactor experiments have indicated the mass of OA  
20 formed in aged BB plumes exceeds the mass of known NMOC precursors, suggesting  
21 unknown NMOC precursors, and/or highlighting the important contribution of semi and  
22 intermediate volatile species to the increase in OA observed (Ortega et al., 2013). Inclusion  
23 of unidentified semi volatile organics in a recent photochemical modelling study of young  
24 BB plumes allowed successful simulation of O<sub>3</sub> and OA, if reasonable assumptions were  
25 made about the chemistry of the unidentified organics (Alvarado et al., 2015).

26 Finally, with increasing global population and urbanisation, it is likely that BB events will  
27 increasingly impact human settlements, either through close proximity of fires or transport of  
28 plumes to urban areas. Consequently a greater understanding is needed of the interactions  
29 between BB and urban emissions. These interactions are complex and have not been  
30 significantly studied to date, although there is evidence that interactions between these two  
31 sources may significantly change the resulting processes and products in plume aging. For  
32 example Jaffe and Wigder (2012), Wigder et al., (2013) and Akagi et al., (2013) show that O<sub>3</sub>  
33 formation is enhanced when NO<sub>x</sub>-limited BB plumes mix with NO<sub>x</sub>- rich urban emissions.

1 Deposition of nitrogen-containing pollutants from major urban areas may also enhance  
2 emission of NO<sub>x</sub> and other nitrogen containing trace gases in BB plumes (Yokelson et al.,  
3 2007). Hecobian et al (2012) found higher concentrations of inorganic aerosol components in  
4 aged BB plumes that had mixed with urban emissions compared to BB plumes, which were  
5 attributed to higher degree of oxidative processing in the mixed plumes.

6 In this study we have investigated the chemical composition of fresh BB plumes in marine air  
7 at the Cape Grim Baseline Air Pollution Station. The BB event occurred unexpectedly during  
8 the Precursors to Particles campaign (Cainey et al., 2007), which aimed to investigate new  
9 particle formation in clean marine air. Despite the opportunistic nature of this work and lack  
10 of targeted BB measurements, a wide variety of trace gas and aerosol species were quantified  
11 which provide valuable information on the composition of BB plumes in this sparsely studied  
12 region of the world.

## 13 **2 Methods**

### 14 **2.1 Cape Grim station location and location of fire**

15 The Cape Grim Baseline Air Pollution Station is located near the north-west tip of the island  
16 state of Tasmania, Australia, 40.7° S latitude and 144.7° E longitude (see Fig 1). The station is  
17 situated on top of a cliff 94 m above mean sea level. When the wind blows from the south  
18 west sector (the Roaring Forties) the air that impacts the station is defined as Baseline and  
19 typically has back trajectories over the Southern Ocean of several days. In northerly wind  
20 directions, urban air from the city of Melbourne some 300 km away is transported across the  
21 ocean (Bass Strait) to the station. North west Tasmania has a mild temperate climate, with  
22 average February temperatures of 15±2° C , RH 75±12%, windspeed of 9±4 m s<sup>-1</sup> (where ±is  
23 1 std dev) and 25 mm precipitation.

24 From 30 January to 24 February 2006 (the Austral late summer), the Precursors to Particles  
25 (P2P) campaign was undertaken (Cainey et al., 2007). On the 15<sup>th</sup> of February 2006, in the  
26 middle of P2P, a fire was ignited on nearby Robbins Island, which lies across farmland 20km  
27 east of Cape Grim. Robbins Island (9748 ha) is separated from the Tasmanian mainland by a  
28 tidal passage 2km across, and has been a freehold property used for the grazing of sheep and  
29 cattle since the 1830s (Buckby, 1988). The vegetation consists of grazed pastures and native  
30 vegetation, mostly disturbed coastal heathland (largely endemic *Epacridaceae*,  
31 *Leptospermum*) and woodland (*Leptospermum*, *Melaleuca* and *Eucalyptus nitida*) with shrubs  
32 interspersed by tussock grasses (*Poa* spp) and sedges (Kitchener and Harris, 2013). The fire

1 burned 2000 ha, mostly coastal heath, over a period of 2 weeks. The vegetation burned is  
2 comparable in structure to the mid and lower story vegetation in Australian temperate forest  
3 and savannah woodland, though lacks the coarse woody debris and the dominant upper story  
4 of trees found particularly in temperate Australian forests. On two occasions an easterly  
5 wind advected the BB plume directly to the Cape Grim Station. The first plume strike (BB1)  
6 occurred from 02:00 – 06:00 (Australian Eastern Standard Time - AEST) on the 16th  
7 February, with light easterly winds of  $3 \text{ m s}^{-1}$  and temperature of  $13 \text{ }^{\circ}\text{C}$  and RH of 96 %. The  
8 second, more prolonged plume strike (BB2) occurred from 23:00 on 23rd February to 05:00  
9 on the 25th February, with strong easterly winds ranging from 10-16  $\text{m s}^{-1}$ , temperatures of  
10 16-22  $^{\circ}\text{C}$  and RH from 75-95 %.

## 11 **2.2 Measurements**

12 During P2P, a number of additional instruments were deployed to run alongside the routine  
13 measurements. All the measurements made during BB1 and BB2 (routine and P2P  
14 measurements) are listed in Table 1, with references supplied for further information. Some  
15 additional information is provided here. All levels of trace gases are expressed as volume  
16 mixing ratios. As the focus of P2P was clean marine air, PM2.5 and PM10 filter samples  
17 were not collected during the BB events.

### 18 2.2.1 NMOCs (PTR-MS)

19 Details on PTR-MS measurements are given in Galbally et al (2007) and some additional  
20 information is provided here.

21 The PTR-MS ran with inlet and drift tube temperature of  $75^{\circ}\text{C}$ , 600V drift tube, 2.2 mbar  
22 drift tube pressure, which equates to an energy field of 140 Td. The  $\text{O}_2^+$  signal was ~2% of  
23 the primary ion  $\text{H}_3\text{O}^+$  signal. The PTR-MS ran in multiple ion detection (MID) mode in  
24 which 26 masses were selected. Masses included in this work were identified by reviewing  
25 instrument intercomparison studies of BB plumes (Christian et al., 2004; Karl et al., 2007b;  
26 de Gouw and Warneke, 2007; Stockwell et al., 2015). Protonated masses were identified as  
27 m/z 28 hydrogen cyanide (HCN), m/z 31 formaldehyde (HCHO), m/z 33 methanol ( $\text{CH}_3\text{OH}$ ),  
28 m/z 42 acetonitrile ( $\text{C}_2\text{H}_3\text{CN}$ ), m/z 45 acetadehyde ( $\text{C}_2\text{H}_4\text{O}$ ), m/z 47 formic acid ( $\text{HCOOH}$ ),  
29 m/z 59 acetone and propanal ( $\text{C}_3\text{H}_6\text{O}$ ), m/z 61 acetic acid ( $\text{CH}_3\text{COOH}$ ), m/z 63 dimethyl  
30 sulphide - DMS ( $\text{C}_2\text{H}_6\text{S}$ ), m/z 69 furan/isoprene ( $\text{C}_4\text{H}_4\text{O}/\text{C}_5\text{H}_8$ ), m/z 71 methacrolein/methyl  
31 vinyl ketone - MVK ( $\text{C}_4\text{H}_6\text{O}$ ), m/z 73 methylglyoxal ( $\text{C}_3\text{H}_4\text{O}_2$ )/methyl ethyl ketone - MEK

1 (C<sub>4</sub>H<sub>8</sub>O), m/z 79 benzene (C<sub>6</sub>H<sub>6</sub>), m/z 85 2-furanone (C<sub>4</sub>H<sub>4</sub>O<sub>2</sub>), m/z 87 2,3-butanedione  
2 (C<sub>4</sub>H<sub>6</sub>O<sub>2</sub>) m/z 93 toluene (C<sub>7</sub>H<sub>8</sub>), m/z 95 phenol (C<sub>6</sub>H<sub>6</sub>O), m/z 107 ethylbenzene + xylenes  
3 (C<sub>8</sub>H<sub>10</sub>), m/z 121 C<sub>3</sub> benzenes (C<sub>9</sub>H<sub>12</sub>), m/z 137 monoterpenes (C<sub>10</sub>H<sub>16</sub>) + unknowns  
4 (C<sub>8</sub>H<sub>8</sub>O<sub>2</sub>). These are expected to be the dominant compounds contributing to these masses.  
5 However, due to the inability of the PTR-MS to differentiate between species with the same  
6 molecular mass, a contribution from other compounds not listed here cannot be ruled out.  
7 Protonated masses m/z 46, m/z 101, m/z 113 and m/z 153 were measured but not identified,  
8 but their concentrations have been reported in this work with the aim of quantifying as much  
9 emitted volatile carbon as possible.

10 During the campaign the PTR-MS was calibrated for the following compounds using  
11 certified gas standards from Scott Specialty Gases, USA and National Physical Laboratory,  
12 UK: methanol, acetaldehyde, acetone, isoprene, MVK and methacrolein, MEK, benzene,  
13 toluene, ethylbenzene, 1,2,4 trimethylbenzene and formaldehyde. Calibration data were used  
14 to construct sensitivity plots which were used to calculate approximate response factors for  
15 other masses not specifically calibrated. Due to having proton affinities similar to water,  
16 formaldehyde and HCN responses are highly dependent on humidity of the sample air. The  
17 changing response of the PTR-MS for these compounds was calculated every 10 minutes by  
18 taking the response of the dry formaldehyde calibration gas, then adjusting this based on the  
19 measured water content of the sample air and relationship between response and humidity as  
20 reported in Inomata et al (2008). Corrections were made to the response of m/z 61 and m/z  
21 137 for known losses due to fragmentation of acetic acid and monoterpenes at those masses.  
22 Dunne et al (2012) reported a significant interference to the acetonitrile signal at m/z 42 from  
23 the <sup>13</sup>C isotopologues of C<sub>3</sub>H<sub>5</sub><sup>+</sup> and the product ion C<sub>3</sub>H<sub>6</sub><sup>+</sup> from reactions involving O<sub>2</sub><sup>+</sup> and  
24 alkanes/alkenes. A detailed correction for this interference was not possible here, due to an  
25 absence of m/z 41, and alkane and alkene measurements. However, during a BB event,  
26 Dunne et al., (2012) calculated a 20% contribution to m/z 42 from non-acetonitrile ions: to  
27 reflect this interference the m/z 42 signal during the BB events has been reduced by 20%.  
28 Minimum detectable limits (MDLs) were calculated according to the principles of ISO 6869  
29 (ISO, 1995) and ranged from 2 – 563 ppt for a one hour measurement. Where measured  
30 levels were below the MDL, a half MDL value was substituted.

31

### 1 **3 Results and discussion**

2 A time series of CO, BC and particle number > 3nm clearly shows the two events (BB1 and  
3 BB2) where plumes from the Robbins Island fire impacted the Cape Grim Station (Fig. 2). A  
4 detailed times series of these two events are presented here, with discussion of the influence  
5 of photochemistry, meteorology and air mass back trajectory on changing composition of  
6 trace gases and aerosol.

#### 7 **3.1 Biomass burning event 1 (BB1) February 16<sup>th</sup> 2006**

##### 8 3.1.1 Brief plume strike, particle growth and ozone enhancement

9 Fig. 3. shows a time series plot from BB1, including both the fresh plume and the changing  
10 composition with changing wind direction. A particle size and number contour plot, wind  
11 direction, O<sub>3</sub>, CO, BC and urban tracer HFC-134a are shown. Periods of interest are labelled  
12 asd Periods A-F (Fig 3.) which are discussed below and summarised in Table 2. Average  
13 particle size distributions for periods corresponding to Periods A-F are presented in Fig. 4.  
14 NMOC data is not available from BB1. The matching air mass back trajectories for periods  
15 corresponding to Periods A-F are shown in Supp Fig. 1a-f.

16 Period A. The fresh BB plume is visible from ~02:00-06:00 (Fig. 3.) through high particle  
17 number concentrations corresponding with elevated CO and BC. The BB particles have a  
18 single, broad size distribution with a dominant mode of 120 nm (Fig. 4a), indicating fresh BB  
19 aerosol (Janhäll et al., 2010). The O<sub>3</sub> mixing ratio during this period is 10 ppb which is lower  
20 than background concentration of about ~15 ppb, likely due to titration by NO emitted from  
21 the fire. The HYSPLIT back trajectory (Supp Fig. 1a) indicates that air which brought the  
22 plume to Cape Grim had previously passed over the north west corner of Tasmania and the  
23 Southern Ocean.

24 Period B. Just after 06:00 (Fig. 3.), a slight wind direction change results in dramatically  
25 reduced particle concentration, CO and BC. The dominant mode of the particles drops from  
26 about 120 nm to 50 nm, but the distribution remains broad and uni-modal (Fig. 4a). From  
27 7:00 – 12:00 there is a gradual increase in the dominant mode of particles from 50 nm to 80  
28 nm suggesting a particle growth event, which is accompanied by an increase in ozone from  
29 12 to 20 ppb. The winds were light (1 m s<sup>-1</sup>) and variable, the temperature mild (19°C) and  
30 skies clear during this period. There is a small enhancement of BC above background  
31 concentrations (12 - 194 ng m<sup>-3</sup>), while the particle size is increasing, suggesting that the

1 station may be on the edge of the plume during this period, however CO is not enhanced  
2 alongside BC and so influence of BB emissions cannot be confirmed. The HYSPLIT  
3 trajectory (Supp Fig. 1b) shows that air arriving at the station is almost entirely of marine  
4 origin but had some contact with the vegetated and sparsely populated North West coast of  
5 Tasmania and appears to pass over Robbins Island before arriving at Cape Grim.

6 Period C. At midday, the dominant particle mode stops increasing and is stable, and BC  
7 drops to background levels. An easterly wind overnight brings air from the sparsely  
8 populated and forested coast of south eastern Australia (Supp Fig. 1 c) which leads to a  
9 further decrease in particle number, but a continued increase in O<sub>3</sub>. The meteorology and  
10 nighttime increase in O<sub>3</sub> is suggestive of a transported continental aged air mass arriving at  
11 Cape Grim, rather than local production. The average particle size distribution over this  
12 period (Fig. 4b) is a single broad distribution with a dominant mode of around 60nm, and is  
13 similar in shape to the distribution during the particle growth event.

14 Period D. A strong urban influence is visible in the early morning on the 17th February (Fig.  
15 3.), when air is transported directly from metropolitan region of Melbourne ~300 km directly  
16 to the north (Supp Fig. 1d). O<sub>3</sub> peaks at ~30 ppb, accompanied by particle number  
17 concentrations of similar magnitude to the direct BB plume the previous day, but without the  
18 elevated CO or BC. The significant urban influence is confirmed by a peak in HFC-134a, an  
19 urban tracer which is widely used in motor vehicle air conditioning and domestic  
20 refrigeration (McCulloch et al., 2003). The average particle size distribution (Fig. 4b) shows  
21 a single broad distribution with a dominant mode of 90 nm.

22 Period E. In mid afternoon on the 17th February a westerly wind from the ocean sector leads  
23 to a sudden drop in HFC-134a, O<sub>3</sub> and particle number. HYSPLIT trajectories suggest the air  
24 mass passed over the ocean for at least 60 hours prior to arriving at Cape Grim (Supp Fig. 1  
25 E). The particle size distribution changes from uni-modal to bi-modal, with dominant modes  
26 at around 50nm and 160 nm (Fig. 4c). This bi-modal distribution is typical of clean marine  
27 air and aerosols are likely dominated by non sea salt sulphate and sea salt particles, which in  
28 the larger mode have been cloud processed (Lawler et al., 2014; Cravigan et al., 2015).

29 Period F. At midnight on the 18th February, (Fig. 3.) terrestrial influence from mainland  
30 Australia is visible (Supp Fig. 1f), with an increase in O<sub>3</sub>, HFC-134a and an increase in  
31 particle number in the 60 – 200nm size range. Over the next 24 hours, decreasing O<sub>3</sub> and  
32 particle number suggests the air is becoming increasingly free of terrestrial influence.

1 However the HYSPLIT trajectory (Supp 1F) shows that some terrestrial influence from  
2 mainland Australia remains for the next 24 hours. This is also shown by HFC-134a values  
3 which are slightly higher than during clean marine period (Event E), and a uni-model average  
4 particle size distribution (Fig. 4c), which resembles the terrestrially-influenced distributions  
5 corresponding to Periods B, C, D and F.

6 It is interesting to note that while size distributions have been described as uni-modal for  
7 Periods B, C, D and F, Fig. 4 a-c shows evidence of a second minor mode at around 160-170  
8 nm in each of these terrestrially-influenced periods. Due to the strong marine influence of the  
9 air arriving at Cape Grim, the 160-170 nm mode in these periods can likely be attributed to  
10 cloud processed non sea salt sulphate and sea salt aerosol, and corresponds to the second  
11 larger mode (160 nm) in the clean marine period of Fig. 3 Period E.

12 Of interest is the contribution that the BB emissions from the Robbins Island fire had on the  
13 O<sub>3</sub> enhancement (Fig. 3). Determining the contribution is challenging given the variety of  
14 emission sources impacting Cape Grim (BB, terrestrial, marine, urban), and understanding  
15 the transport and mixing of these emissions. During BB1 The HFC-134a indicates an  
16 increasing influence from urban air from mainland Australia (indicating a likely source of O<sub>3</sub>  
17 or O<sub>3</sub> precursors), and indeed the O<sub>3</sub> and HFC-134a concentrations do increase in parallel  
18 (Fig. 3). However, some of the increases in O<sub>3</sub> occurred when there was minimal urban  
19 influence, for example during the particle growth event (Fig. 3 Period B), and may have been  
20 driven by emissions from the local fire. Use of a chemical transport model to determine  
21 influence of fire emissions on O<sub>3</sub> formation will be reported in a follow up paper by Lawson  
22 et al (2015).

23

### 24 3.1.2 Ability of particles in BB event 1 (BB1) to act as CCN

25 The ability of particles to act as CCN at 0.5% supersaturation was investigated during the  
26 fresh BB plume (Fig. 3 Period A) and the particle growth period (Period B). The CCN  
27 activity of particles was also calculated during the 24 hours of Period F, chosen due to the  
28 absence of BB tracers during this period, and predominance of marine air with some minor  
29 terrestrial influence. The average hourly ratio of CCN number to condensation nuclei (CN)  
30 number > 80 nm (CN80, measured using the SMPS) was calculated. CN80 was chosen based  
31 on a study by Petters et al., (2009) which suggested even weakly hygroscopic BB aerosols  
32 began to activate to CCN at a diameter of approximately 80 nm and larger. Given this, any

1 observed difference in the CCN/CN80 ratio may then be due to either different chemical  
2 composition between the particles, and/or differences in particles size distributions, as larger  
3 particles are more easily activated to CCN. The CCN/CN80 ratio has only been calculated  
4 for BB1 because there are no aerosol size distribution measurements (and hence no CN80  
5 measurements) for BB2.

6 Fig. 5a shows the CCN/CN80 expressed as a percentage for the fresh plume (Period A),  
7 particle growth event (Period B), and background marine/terrestrial (Period F). Error bars are  
8  $\pm 1$  standard error of the mean. Fig. 5b shows the absolute number concentration of CCN  
9 during these periods.

10 The CCN/CN80 ratio during the fresh BB plume strike (Period A) is  $56 \pm 8\%$ . Petters et al.,  
11 (2009) show that in laboratory BB measurements the CCN activation of 80 nm particles  
12 ranges from a few % for low or weakly hygroscopic fuels to up to 60% for more hygroscopic  
13 fuels such as chamise, suggesting that the particles produced from coastal heath burned here  
14 may be more hygroscopic than those from other fuel types.

15 The CCN/CN80 ratio is substantially higher during the particle growth event (Period B)  
16 ( $77 \pm 4\%$ ). Fig. 4a shows that the average dominant diameter of particles shifts from around  
17 120 nm during Period A to around 60nm during Period B. The smaller diameter during  
18 Period B suggests that particle size is not the reason for the increased CCN/CN80 ratio during  
19 the particle growth period, but is likely due to a changing chemical composition of particles  
20 between the two periods, with more hygroscopic particles measured during the particle  
21 growth period compared to the fresh BB particles. Volatility and hygroscopicity  
22 measurements of particles are available from Period A using a volatility and hygroscopic  
23 tandem differential mobility analysis (VH-TDMA) system (Fletcher et al., 2007). These  
24 measurements focused on the composition of 60 nm particles, and suggested they consisted  
25 of a non-hygroscopic 23-nm core, a hygroscopic layer to 50 nm and a hydrophobic outer  
26 layer to 60 nm (possible homogeneously mixed). There was some evidence that the particle  
27 core contained two different types of particle, possibly due to merging of marine and BB  
28 particles. The suggested mix of hygroscopic and non-hygroscopic materials in fresh BB  
29 particles is in agreement with the fact that only 56% of these particles were hygroscopic  
30 enough to act as CCN. While the composition of the fresh BB particles may only be inferred  
31 from these measurements, the non-hygroscopic core may be black carbon or primary organic  
32 aerosol, the hygroscopic component an inorganic material such as sea salt or ammonium  
33 nitrate or sulphate or a hydroscopic organic such as MSA which is abundant in the marine

1 boundary layer at Cape Grim in summer. The hydrophobic outer layer may be a hydrocarbon-  
2 type organic, with a low O:C ratio, which was co-emitted in the fire and condensed on to the  
3 particle as the plume cooled and was transported to Cape Grim (Fletcher et al., 2007).  
4 Unfortunately no hygroscopicity or volatility measurements are available from Period B  
5 (particle growth).  
6 During background marine Period F, all ( $104 \pm 3\%$ ) of the particles  $>80$  nm could act as CCN  
7 (Fig. 5a). A value of more than 100% is not physically possible but is due to uncertainty  
8 associated with the different techniques (SMPS and CCN) and measurement synchronisation.  
9 This result is in agreement with the work of Fletcher et al (2007) who reported that the fresh  
10 BB particles from BB1-A had a lower hygroscopic growth factor than marine particles. Fig.  
11 4 a and 4 c shows the average size distribution of particles during Period F (background  
12 marine/terrestrial) is very similar to period B (particle growth), despite the air masses coming  
13 from different directions (westerly and easterly respectively). As discussed previously, both  
14 these periods have a predominant marine back trajectory and some terrestrial influence. It is  
15 therefore likely that the main difference between the particle composition between these two  
16 periods, and the reason for the lower CCN/CN ratio during Period B is the presence of non or  
17 weakly-hygroscopic  $>80$  nm particles, such as the BC which elevated above background  
18 levels during Period B.  
19 Sea salt and non sea salt sulphate aerosol are important sources of CCN in the marine  
20 boundary layer (Korhonen et al., 2008; Quinn and Bates, 2011) and are likely the main source  
21 of CCN in Period F (and possibly Period B). The fact that all particles  $>80$ nm could act as  
22 CCN in Period F suggests that any non-hygroscopic terrestrial particles which reached Cape  
23 Grim during this time were likely to have been aged and oxidised during the several hundred  
24 kms during transport from the mainland.  
25 Finally, the absolute number concentration of CCN in the fresh plume (A) (hourly average)  
26 was  $\sim 2000$   $\text{cm}^{-3}$  (Fig. 5b), with minute average concentrations up to  $\sim 5500$   $\text{CCN cm}^{-3}$ . In  
27 contrast, the average number of CCN during particle growth (Period B) was a factor of 3  
28 lower at  $\sim 700$   $\text{CCN cm}^{-3}$ . During the background marine/terrestrial Period (F) in BB1, the  
29 CCN is  $320$   $\text{CCN cm}^{-3}$ , with low variability, a value which is within the range of typical  
30 pristine marine values (Gras, 2007). Overall, CCN were enhanced by a factor  $\sim 6$  and a factor  
31 of  $\sim 30$  above background levels in BB1 and BB2 respectively (see Sect. 3.2 and Table 3).  
32 Despite the modest ability of fresh BB particles to form CCN (CCN/CN<sub>80</sub> ratio of 56%), the  
33 very high numbers of particles ejected into the marine boundary layer during the fire

1 highlights the dramatic impact BB plumes can have on the CCN population, particularly in  
2 clean marine regions.

3

## 4 **3.2 BB event 2 (BB2) February 23<sup>rd</sup> 2006**

### 5 3.2.1 Interplay between emissions, meteorology and sources

6 BB2 was of much longer duration than BB1, and lasted about 29 hours. Fig. 6 shows a time  
7 series including wind direction and rainfall, O<sub>3</sub>, CO, BC, BB tracer acetonitrile,  
8 acetonitrile/CO ratio (where CO > 400 ppb) and urban tracer HFC-134a. Periods of interest  
9 are highlighted as A-D (Fig 6.), summarised in Table 2 and discussed below. Particle size  
10 distribution data is not available for BB2. The matching air mass back trajectories for the  
11 events highlighted in Fig. 6. are shown in Supplementary Fig. 2. a-d.

12 Period A. For the first 24 hours of BB2, there is clear elevation in CO, BC and acetonitrile,  
13 due to the easterly wind advecting the plume directly to Cape Grim. The acetonitrile mixing  
14 ratio is ~ 1 ppb and is enhanced by a factor of 30 above typical background levels at Cape  
15 Grim of ~35 ppt (Table 3). The acetonitrile ratio to CO is also relatively constant during this  
16 time (1-2 ppt/ppb). An ozone peak of 27 ppb (minute data) occurs in mid afternoon on 24  
17 February, corresponding to an hourly Normalised Excess Mixing Ratio (NEMR)  $\Delta O_3/\Delta CO$   
18 of 0.05 (where NEMR is an excess mixing ratio normalised to a non-reactive co-emitted  
19 tracer, in this case CO, see Akagi et al., 2011).

20 Period B. At 04:00 on 25th February acetonitrile peaks by a factor of 17 over 2 hours (Fig. 6  
21 Period B) with a smaller peak at 23:00 on the 24th February. Almost all masses on the PTR-  
22 MS increased at the same time as acetonitrile, including masses corresponding to HCN,  
23 methanol, acetaldehyde, acetone, furan/isoprene and benzene). The corresponding CO peak at  
24 04:00 (~1500 ppb) increased by a factor of 21 and is the largest peak from BB2. The  
25 corresponding BC peak at 04:00 is much smaller than peaks which occurred earlier in BB2.  
26 This large enhancement in CO and NMOCs but modest enhancement in BC suggests a  
27 decrease in the combustion efficiency during this time. This is further supported by increases  
28 in the ratio of acetonitrile to CO (where CO > 400 ppb) by a factor of ~3 during the peak  
29 periods (Fig. 6), and a decrease in the ratios of BC to CO during peak periods (average  $0.9 \pm$   
30  $0.3 \text{ ng m}^{-3} \text{ ppb}^{-1}$ ) compared to non-peak periods ( $2.2 \pm 0.1 \text{ ng m}^{-3} \text{ ppb}^{-1}$ ).

1 A small amount of rainfall recorded at Cape Grim (1.4 mm) corresponds with the second  
2 peak (Fig. 6). Archived radar images from the Bureau of Meteorology (West Takone 128 km,  
3 10 min resolution) confirm that very light patchy rain showers occurred on Robbins Island at  
4 23:10 followed by intermittent rain showers of light to moderate intensity from 12:40 until  
5 05:40, on the 25th February (S. Baly, pers com). The total rainfall amount that fell on  
6 Robbins Island was between 1-5 mm ([www.bom.gov.au](http://www.bom.gov.au)). Evidence of rainfall coinciding  
7 with an enhancement in NMOC ER to CO, and a decrease in BC ER to CO suggests that the  
8 rainfall changed the combustion processes of the fire. The enhanced ERs of NMOCs to CO  
9 which are associated with low-efficiency, smouldering combustion, can therefore attributed  
10 to a short term decrease in combustion efficiency, driven by rainfall. Due to the small  
11 number of data points (2) it is not possible to calculate reliable ER to CO during this  
12 shortlived event. But this time series highlights the importance of relatively minor  
13 meteorological events on BB emission ratios.

14 While the elevated concentrations of BB tracers CO, BC and acetonitrile during this period  
15 are attributed to emissions from the local fire, back trajectories (Supp Fig. 3B) show that air  
16 arriving at Cape Grim had previously passed over the Australian mainland. The increasing  
17 anthropogenic influence is also supported by increasing levels of HFC-134a and a  
18 corresponding increase in O<sub>3</sub> which peaks at 34 ppb (minute data) at 1:00-2:00, with an  
19 hourly NEMR for  $\Delta O_3/\Delta CO$  of 0.07 (the highest observed).

20 Period C. With a change in wind direction further to the north from 5:00 onwards (Fig. 6),  
21 BB tracers BC, CO and acetonitrile all decrease to background levels, indicating fire  
22 emissions are no longer impacting the station. Ozone begins to increase at 8:00 and reaches  
23 ~40 ppb 3 hours later, corresponding with a maximum HFC-134a mixing ratio of ~ 35 ppt.  
24 The air mass back trajectory (Supp Fig. 2 C) confirms that air from Melbourne is impacting  
25 the station during this period

26 Period D. As wind moves further into the west in to the clean marine sector (Supp Fig. 2D),  
27 O<sub>3</sub> and HFC-134a decrease to background levels.

28 This time series highlights possible interplay of sources and meteorology on the observed  
29 trace gases and particles. The very large increase of NMOCs and CO observed during the  
30 rainfall period shows the potentially large affect of quite minor meteorological events on BB  
31 emission ratios. While other studies have found a link between fuel moisture, MCE and  
32 emissions of PM<sub>2.5</sub>, (eg Watson et al., 2011 ; Hosseini et al., 2013) this is the first study to

1 our knowledge which has linked rainfall with a large increase in trace gas emission ratios  
2 from BB.

3 This work also highlights the large influence that BB plumes can have on the composition of  
4 air in the marine boundary layer. During the direct plume strikes, absolute numbers of  
5 particles > 3nm increased from 600 to 25,000 particles cm<sup>-3</sup> (hourly average). In BB2, as was  
6 the case in BB1, the O<sub>3</sub> concentrations closely correspond with the HFC134a concentrations.  
7 This suggests that transport of photochemically processed air from urban areas to Cape Grim  
8 is the main driver of the O<sub>3</sub> observed but does not rule out possible local O<sub>3</sub> formation from  
9 BB emissions. NEMRs of  $\Delta\text{O}_3/\Delta\text{CO}$  ranged from 0.001-0.074 during BB2 which are  
10 comparable to NEMRs observed elsewhere in BB plumes <1 hr old (Yokelson et al.,  
11 2003;Yokelson et al., 2009).

### 12 3.2.2 Chemical composition of BB2 and selection of in-plume and 13 background periods

14 The composition of the fresh plume during BB2 was explored by determining for which trace  
15 gas and aerosol species the enhancement above background concentrations was statistically  
16 significant. Emission ratios (ER) and particle number to CO were then calculated for these  
17 selected species and converted to emission factors (EF).

18 The first 10 hours of Period A from BB2 (from 23:00 on the 23<sup>rd</sup> Feb to 09:00 on the 24<sup>th</sup>  
19 Feb) was selected to characterise the fresh plume composition. During this time, the air which  
20 brought the Robbins Island BB emissions to Cape Grim had previously passed over the ocean  
21 and so was free of terrestrial or urban influence (NOAA HYSPLIT Supp Fig. 2A). While  
22 fresh BB emissions were measured at Cape Grim beyond 10:00 on the 24<sup>th</sup> Feb, the air at this  
23 time had prior contact with the Australian mainland, including the Melbourne region and so  
24 was considered unsuitable for characterising the BB plume. During the selected time period,  
25 wind speeds of 16 m s<sup>-1</sup> meant that the plume travelled the 20 km to Cape Grim over a period  
26 of about 20 minutes, which allows the plume to cool to ambient temperatures but ensured  
27 minimum photochemical processing of the plume (Akagi et al., 2011). Advection of the  
28 plume to the site occurred primarily at night so minimal impact of photochemical reactions  
29 on the plume composition is expected (Vakkari et al., 2014). It is therefore assumed that the  
30 enhancement ratios measured at Cape Grim during this time are unaltered from the original  
31 emission ratios. Finally, photos indicate the Robbins Island fire plume was well mixed within

1 the boundary layer and was not lofted into the FT, allowing representative ‘fire-averaged’  
2 measurements to be collected (Akagi et al., 2014).

3 Background concentrations of gas and particle species were determined from fire-free periods  
4 in early March 2006 which had a very similar air back trajectory to trajectories during the fire  
5 (not shown). Concentrations of long lived urban tracers (not emitted from fires) including  
6 HFC-32, HFC-125a and HFC-134a were also used to match suitable background time periods  
7 with the fresh plume period.

8 Table 3 lists the gas and aerosol species measured, whether concentrations were statistically  
9 higher in the plume compared to background air, average background concentrations, average  
10 in-plume concentrations, emission ratios (ER) to CO and EF ( $\text{g kg}^{-1}$ ). Details of ER and EF  
11 calculations are given below. Hourly average data were used for these calculations.

### 12 3.2.3 Species emitted in BB event 2 (BB2) –t tests

13 Hypothesis testing using the student t tests (one sided) were carried out to determine whether  
14 concentrations in the BB plume ( $x_1$ ) were significantly higher than concentrations observed in  
15 the background periods ( $x_2$ ), with a 95% level of significance. Table 3 shows which species  
16 were statistically enhanced in the BB plume, and hence assumed to be emitted from the fire  
17 ( $x_1-x_2>0$ ) and those which were not statistically enhanced in the BB plume ( $x_1-x_2=0$ ). While  
18 the vast majority of species measured were found to be significantly enhanced in the BB  
19 plume, there were a number of species including DMS, chloroform, methyl chloroform,  
20 dichloromethane, carbon tetrachloride, bromoform and the urban tracers HFC-032, HFC-125  
21 and HFC-134a which were not significantly enhanced. DMS has consistently been found to  
22 be emitted from BB in many studies (as summarised by Akagi et al 2011). However, in this  
23 study due to close proximity to the ocean, the likely emission of DMS from the BB was likely  
24 obscured by the high variability in the background concentration. The absence of emission of  
25 chloroform, methyl chloroform, dichloromethane, carbon tetrachloride, tribromomethane and  
26 the HFCs are in agreement with a recent study of boreal forest emissions by Simpson et al  
27 (2011).

### 28 3.2.4 Calculation of Emission Ratios to CO

29 Excess mixing ratios ( $\Delta x$ ) were calculated for species that were statistically higher in the  
30 plume compared to background air by subtracting background mixing ratios from the hourly  
31 in-plume mixing ratios. Emission ratios to CO were then calculated by plotting  $\Delta x$  versus

1  $\Delta\text{CO}$ , fitting a least squares line to the slope and forcing the intercept to zero (Yokelson et al.,  
2 1999). Emission ratios (ER) to CO and the  $R^2$  of the fit are reported in Table 3.

3 The excess mixing ratios of all species significantly enhanced in the plume correlated with  
4 the excess mixing ratios of CO with an  $R^2$  value of  $\geq 0.4$ , with the exception of  $\text{CO}_2$ , HCHO,  
5 HCOOH, m/z 101,  $\text{N}_2\text{O}$ , and CCN number concentration (see discussion below and Fig. 3b).  
6 ER plots for BC,  $\text{CN}>3\text{nm}$ ,  $\text{H}_2$ ,  $\text{CH}_4$ ,  $\text{C}_2\text{H}_6$ ,  $\text{C}_6\text{H}_6$ ,  $\text{CH}_3\text{COOH}$ ,  $\text{C}_6\text{H}_6\text{O}$  and  $\text{C}_2\text{H}_3\text{N}$  are shown  
7 in Fig. 7. The ER of CO to particle number ( $38 \text{ cm}^{-3} \text{ ppb}^{-1}$ ) agrees well with a literature  
8 averaged value of  $34 \pm 16 \text{ cm}^{-3} \text{ ppb}^{-1}$  (Janhall., et al 2010). The  $\text{H}_2$  ER to CO (0.10) is lower  
9 than the range reported from BB emissions (0.15-0.45), as summarised by Vollmer et al.,  
10 (2012).

11 There is a low correlation between mixing ratios of CO and  $\text{CO}_2$  (ER to CO  $R^2 = 0.15$ , see  
12 Table 3). This is in part because CO and  $\text{CO}_2$  are emitted in different ratios from different  
13 combustion processes (smouldering and flaming respectively) and may also be influence by  
14 variability in background levels of  $\text{CO}_2$  (Andreae et al., 2012). Of the other species with  $R^2$   
15 values of  $<0.4$ , HCHO and HCOOH are both emitted directly from BB, but are also oxidation  
16 products of other species co-emitted in BB. It is therefore possible that in the 20 minute  
17 period between plume generation and sampling, chemical processing has lead to generation  
18 of these compounds in the plume, which has changed the ER to CO. In addition, sampling  
19 losses of HCOOH down the inlet line are possible (Stockwell et al., 2014). The lack of  
20 relationship between  $\Delta\text{CO}$  and  $\Delta\text{N}_2\text{O}$  is likely because  $\text{N}_2\text{O}$  is an intermediate oxidation  
21 product which is both formed and destroyed during combustion. Studies of emissions from  
22 Savanna burning in Northern Australia have found  $\text{N}_2\text{O}$  to be insensitive to changes in MCE  
23 (Meyer and Cook, 2015; Meyer et al., 2012; Volkova et al., 2014). A further reason for a lack  
24 of correlation with  $\Delta\text{CO}$  for  $\Delta\text{N}_2\text{O}$  is that as for  $\text{CO}_2$ , the plume enhancement of  $\Delta\text{N}_2\text{O}$  is  
25 relatively small compared to the observed variability in background concentrations. Finally  
26 the lack of correlation between  $\Delta\text{CCN}$  and  $\Delta\text{CO}$  may be due interaction of plume aerosol  
27 with background sources of CCN, such as sea salt, and the change in particle properties and  
28 composition in the 20 minutes after emission.

29

### 30 3.2.5 Calculation of MCE and EF and comparison with other studies

31 Combustion efficiency (CE) is a commonly used measure of the degree of oxidation of fuel  
32 carbon to  $\text{CO}_2$ . Combustion efficiency is commonly approximated as the modified

1 combustion efficiency (MCE) (Yokelson et al., 1999), which is calculated using the  
2 following equation

$$3 \quad MCE = \frac{\Delta CO_2}{\Delta CO_2 + \Delta CO} \quad (1)$$

4 In this study the 10 hour integrated MCE was 0.88, which indicates predominantly  
5 smouldering combustion. The ER of BC to CO reported here is in good agreement with BC  
6 to CO ERs in smouldering fires (MCE <0.9) reported by Kondo et al., (2011) and May et al.,  
7 (2014) which suggests that the excess CO<sub>2</sub>, and MCE has been determined reliably.

8 Whole of fire Emission factors were calculated according to the Carbon Mass Balance  
9 method (Ward and Radke, 1993). Emission factors were calculated relative to combusted fuel  
10 mass (Andreae and Merlet, 2001), assuming 50% fuel carbon content by dry weight  
11 according to the following equation.

$$12 \quad EF_x(g/kg) = \frac{[\Delta x]}{\sum([\Delta CO_2] + [\Delta CO] + [\Delta CH_4])} \times 0.5 \times 1000(g/kg) \times \frac{MW(x)}{12} \quad (2)$$

13 The Carbon Mass Balance method assumes all volatilised carbon is detected, including CO<sub>2</sub>,  
14 CO, hydrocarbons and particulate carbon. Here the major volatile carbon components of CO<sub>2</sub>,  
15 CO and CH<sub>4</sub> were used in the EF calculation, so the resulting EF may be overestimated by 1-  
16 2 % (Andreae and Merlet, 2001).

17 For comparison with the carbon mass balance method, EF were also calculated using an  
18 average CO EF for temperate forests from Akagi et al (2011), which corresponds to an MCE  
19 of 0.92 (see Supplementary material for EF and method details). Trace gas EF calculated  
20 using an assumed CO EF were generally 50% lower than EF calculated using the carbon  
21 mass balance method.

22 Table 4 shows EFs calculated from this study (Carbon Mass Balance Method) compared with  
23 other Australian BB studies both of eucalypt and sclerophyll forest fires in temperate south  
24 eastern Australia (Paton-Walsh et al., 2005; Paton-Walsh et al., 2008; Paton-Walsh et al.,  
25 2014), and tropical savanna fires in northern Australia (Paton-Walsh et al., 2010; Meyer et  
26 al., 2012; Hurst et al., 1994a; Hurst et al., 1994b; Shirai et al., 2003; Smith et al., 2014). The  
27 fire in this study (41°S) is >1000 km south of the temperate forest fires used for comparison  
28 (33-35°S), and some 2500 km South East of the tropical savannah fires in the comparison  
29 (12-14°S).

1 EF from this study reported in Table 4 are within 50% of the EFs from the other South  
2 Eastern Australian studies except for acetic acid, which is 5 times lower than the EF reported  
3 by Paton-Walsh et al., (2014). EF from this study are also within 50% of temperate NH EF  
4 (temperate forests and chaparral) except for hydrogen, acetic acid and the methyl halides and  
5 within 80% of the average tropical savannah EF, with the exception of acetic acid and the  
6 methyl halides.

7 The acetic acid EF from this study is significantly lower than reported from Australian and  
8 NH temperate studies, though the variability reported elsewhere is large. Acetic acid may  
9 form rapidly in BB plumes (Akagi et al., 2012), which adds uncertainty to the EF in plumes  
10 which are sampled some distance downwind of emission. The lower EF reported in this work  
11 may be due to inlet losses, or another loss process such as nocturnal uptake of acetic acid on  
12 to wet aerosols (Stockwell et al., 2014).

13 The methyl halides EF from this study are in the same proportion as seen elsewhere (i.e. EF  
14 ( $\text{CH}_3\text{Cl}$ ) > EF( $\text{CH}_3\text{Br}$ ) > EF( $\text{CH}_3\text{I}$ )) but the EF magnitudes are substantially higher. The  
15  $\text{CH}_3\text{Cl}$  EF from this study is more than a factor of 4 higher than elsewhere in Australia and  
16 the NH, the  $\text{CH}_3\text{Br}$  EF between 5 and 11 times higher and  $\text{CH}_3\text{I}$  EF a factor of about 3 times  
17 higher than elsewhere. EF calculated by the alternative ER to CO method (Supplementary  
18 material) gives methyl halide EFs which are 30% lower but still much larger than those  
19 observed elsewhere. It is likely that the high methyl halide EFs reported here are due to high  
20 halogen content of soil and vegetation on the island, due to very close proximity to the ocean,  
21 and transfer of halogens to the soil via sea spray (McKenzie et al., 1996). Chlorine and  
22 bromine content in vegetation has been shown to increase with proximity to the coast  
23 (McKenzie et al., 1996; Stockwell et al., 2014) and methyl chloride and hydrochloric acid EF  
24 are impacted by the chlorine content of vegetation (Reinhardt and Ward, 1995; Stockwell et  
25 al., 2014).

#### 26 **4 Summary and future work**

27 The opportunistic measurement of BB plumes at Cape Grim Baseline Air Pollution Station in  
28 February 2006 has allowed characterisation of BB plumes in a region with few BB  
29 measurements. Plumes were measured on two occasions (events BB1 and BB2) when the  
30 plume was advected to Cape Grim from a fire on Robbins Island some 20 km to the east.

31 The fresh plume had a large impact on the number of particles at Cape Grim, with absolute  
32 numbers of particles > 3 nm increasing from  $600 \text{ cm}^{-3}$  in background air up to  $25,000 \text{ cm}^{-3}$

1 during the fresh plume in BB2 (hourly average) and CCN increasing from  $160 \text{ cm}^{-3}$  in  
2 background air up to  $5500 \text{ cm}^{-3}$  (hourly average). The dominant particle diameter mode  
3 measured in BB1 was 120 nm.

4 After a slight wind direction change, BB tracers BC and CO decreased dramatically and the  
5 dominant particle mode decreased to 50nm. A gradual increase in particle size to 80nm was  
6 observed over 5 hours, in calm sunny conditions, alongside a modest increase in ozone. BC  
7 was present above background levels during particle growth but CO was not significantly  
8 elevated, so the presence of the fire emissions during particle growth cannot be determined. .  
9 During BB1, the ability of particles  $> 80\text{nm}$  to act as CCN at 0.5% supersaturation was  
10 investigated, including during the fresh BB, particle growth and background  
11 terrestrial/marine periods. The  $\Delta\text{CCN}/\Delta\text{CN}_{80}$  ratio was lowest during the fresh BB plume  
12 strike ( $56\pm 8\%$ ), higher during the particle growth event ( $77\pm 4\%$ ) and is higher still ( $104\pm 3\%$ )  
13 in background marine air.

14 Enhancements in  $\text{O}_3$  concentration above background were observed following the direct  
15 plume strikes in BB1 and during the direct plume strike in BB2, with NEMRs ( $\Delta\text{O}_3/\Delta\text{CO}$ ) of  
16 0.001-0.074. It is likely that some of the  $\text{O}_3$  enhancement that occurred during the particle  
17 growth event in BB1 was driven by fire emissions. However on other occasions enhancement  
18 of  $\text{O}_3$  which occurred at night, corresponding with enhancements of urban tracer HFC-134a  
19 was most likely due to air being transported from mainland Australia. Chemical transport  
20 modelling will be used in a follow up paper to elucidate the sources, and where possible the  
21 species responsible for the  $\text{O}_3$  enhancement and change in particle hygroscopicity observed,  
22 as well as the age of the urban emissions transported from Melbourne.

23 The more prolonged BB2 allowed determination of emission ratios (ER) to CO and Emission  
24 Factors (EF) for a range of trace gas species, CN and BC using the carbon mass balance  
25 method. These EF, which were calculated from nocturnal measurements of the BB plume,  
26 provide a unique set of emission estimates for a wide range of trace gases from burning of  
27 coastal heathland in temperate Australia.

28 A very large increase in emissions of NMOCs (factor of 16) and CO (factor of 21), and a  
29 more modest increase in BC (factor of 5) occurred during BB2. The ratio of acetonitrile to  
30 CO increased by a factor of 2-3 and the ratio of BC to CO halved during this period. This  
31 change in emission ratios is attributed to decreased combustion efficiency during this time,  
32 due to rainfall over Robbins Island. Given that air quality and climate models typically use a

1 fixed EF for trace gas and aerosol species, the impact of varying emissions due to  
2 meteorology may not be captured by models.

3 More broadly, given the high variability in reported EF for trace gas and aerosol species in  
4 the literature, the impact of EF variability on modelled outputs of both primary BB species  
5 (i.e. CO, BC, NMOCs) and secondary BB species (i.e. O<sub>3</sub>, oxygenated NMOCs, secondary  
6 aerosol) is likely to be significant. In the next phase of this work, in addition to exploring the  
7 chemistry described above with chemical transport modelling, we will also systematically  
8 explore the sensitivity of these models to EF variability, as well as spatial and meteorological  
9 variability.

10

### 11 **Acknowledgements**

12 The Cape Grim program, established by the Australian Government to monitor and study  
13 global atmospheric composition, is a joint responsibility of the Bureau of Meteorology  
14 (BOM) and the Commonwealth Scientific and Industrial Research Organisation (CSIRO).  
15 We thank the staff at Cape Grim and staff at CSIRO Oceans and Atmosphere (Rob Gillett,  
16 Suzie Molloy) for their assistance and input. We acknowledge the NOAA Air Resources  
17 Laboratory (ARL) for the provision of the HYSPLIT transport and dispersion model used in  
18 this publication. West Takone radar images courtesy of Stuart Baly (BOM). We thank both  
19 reviewers for insightful comments and suggestions which have been incorporated into the  
20 manuscript.

21

## 1 **References**

- 2 Akagi, S. K., Yokelson, R. J., Wiedinmyer, C., Alvarado, M. J., Reid, J. S., Karl, T., Crouse,  
3 J. D., and Wennberg, P. O.: Emission factors for open and domestic biomass burning for use  
4 in atmospheric models, *Atmospheric Chemistry and Physics*, 11, 4039-4072, 10.5194/acp-11-  
5 4039-2011, 2011.
- 6 Akagi, S. K., Craven, J. S., Taylor, J. W., McMeeking, G. R., Yokelson, R. J., Burling, I. R.,  
7 Urbanski, S. P., Wold, C. E., Seinfeld, J. H., Coe, H., Alvarado, M. J., and Weise, D. R.:  
8 Evolution of trace gases and particles emitted by a chaparral fire in California, *Atmospheric*  
9 *Chemistry and Physics*, 12, 1397-1421, 10.5194/acp-12-1397-2012, 2012.
- 10 Akagi, S. K., Yokelson, R. J., Burling, I. R., Meinardi, S., Simpson, I., Blake, D. R.,  
11 McMeeking, G. R., Sullivan, A., Lee, T., Kreidenweis, S., Urbanski, S., Reardon, J., Griffith,  
12 D. W. T., Johnson, T. J., and Weise, D. R.: Measurements of reactive trace gases and variable  
13 O<sub>3</sub> formation rates in some South Carolina biomass burning plumes, *Atmos. Chem. Phys.*,  
14 13, 1141-1165, 10.5194/acp-13-1141-2013, 2013.
- 15 Akagi, S. K., Burling, I. R., Mendoza, A., Johnson, T. J., Cameron, M., Griffith, D. W. T.,  
16 Paton-Walsh, C., Weise, D. R., Reardon, J., and Yokelson, R. J.: Field measurements of trace  
17 gases emitted by prescribed fires in southeastern US pine forests using an open-path FTIR  
18 system, *Atmospheric Chemistry and Physics*, 14, 199-215, 10.5194/acp-14-199-2014, 2014.
- 19 Alvarado, M. J., Lonsdale, C. R., Yokelson, R. J., Akagi, S. K., Coe, H., Craven, J. S.,  
20 Fischer, E. V., McMeeking, G. R., Seinfeld, J. H., Soni, T., Taylor, J. W., Weise, D. R., and  
21 Wold, C. E.: Investigating the links between ozone and organic aerosol chemistry in a  
22 biomass burning plume from a prescribed fire in California chaparral, *Atmos. Chem. Phys.*,  
23 15, 6667-6688, 10.5194/acp-15-6667-2015, 2015.
- 24 Andreae, M. O., and Merlet, P.: Emission of trace gases and aerosols from biomass burning,  
25 *Global Biogeochemical Cycles*, 15, 955-966, 10.1029/2000gb001382, 2001.
- 26 Andreae, M. O., Artaxo, P., Brandao, C., Carswell, F. E., Ciccioli, P., da Costa, A. L., Culf,  
27 A. D., Esteves, J. L., Gash, J. H. C., Grace, J., Kabat, P., Lelieveld, J., Malhi, Y., Manzi, A.  
28 O., Meixner, F. X., Nobre, A. D., Nobre, C., Ruivo, M., Silva-Dias, M. A., Stefani, P.,  
29 Valentini, R., von Jouanne, J., and Waterloo, M. J.: Biogeochemical cycling of carbon, water,  
30 energy, trace gases, and aerosols in Amazonia: The LBA-EUSTACH experiments, *Journal of*  
31 *Geophysical Research-Atmospheres*, 107, 8066, 10.1029/2001jd000524, 2002.
- 32 Andreae, M. O., Artaxo, P., Beck, V., Bela, M., Freitas, S., Gerbig, C., Longo, K., Munger, J.  
33 W., Wiedemann, K. T., and Wofsy, S. C.: Carbon monoxide and related trace gases and  
34 aerosols over the Amazon Basin during the wet and dry seasons, *Atmospheric Chemistry and*  
35 *Physics*, 12, 6041-6065, 10.5194/acp-12-6041-2012, 2012.
- 36 Buckby, P.: Robbins Island Saga, The Commercial Finance Company of Tasmania Pty Ltd,  
37 Smithton Tasmania, 1988.
- 38 Cainey, J. M., Keywood, M., Grose, M. R., Krummel, P., Galbally, I. E., Johnston, P., Gillett,  
39 R. W., Meyer, M., Fraser, P., Steele, P., Harvey, M., Kreher, K., Stein, T., Ibrahim, O.,  
40 Ristovski, Z. D., Johnson, G., Fletcher, C. A., Bigg, E. K., and Gras, J. L.: Precursors to  
41 Particles (P2P) at Cape Grim 2006: campaign overview, *Environmental Chemistry*, 4, 143-  
42 150, 10.1071/en07041, 2007.
- 43 Christian, T. J., Kleiss, B., Yokelson, R. J., Holzinger, R., Crutzen, P. J., Hao, W. M.,  
44 Saharjo, B. H., and Ward, D. E.: Comprehensive laboratory measurements of biomass-

1 burning emissions: 1. Emissions from Indonesian, African, and other fuels, *Journal of*  
2 *Geophysical Research-Atmospheres*, 108, 10.1029/2003jd003704, 2003.

3 Christian, T. J., Kleiss, B., Yokelson, R. J., Holzinger, R., Crutzen, P. J., Hao, W. M., Shirai,  
4 T., and Blake, D. R.: Comprehensive laboratory measurements of biomass-burning  
5 emissions: 2. First intercomparison of open-path FTIR, PTR-MS, and GC- MS/FID/ECD,  
6 *Journal of Geophysical Research-Atmospheres*, 109, 12, D02311  
7 10.1029/2003jd003874, 2004.

8 Cravigan, L. T., Ristovski, Z., Modini, R. L., Keywood, M. D., and Gras, J. L.: Observation  
9 of sea salt fraction in sub-100 nm diameter particles at Cape Grim, *Journal of Geophysical*  
10 *Research: Atmospheres*, 2014JD022601, 10.1002/2014JD022601, 2015.

11 Cubison, M. J., Ortega, A. M., Hayes, P. L., Farmer, D. K., Day, D., Lechner, M. J., Brune,  
12 W. H., Apel, E., Diskin, G. S., Fisher, J. A., Fuelberg, H. E., Hecobian, A., Knapp, D. J.,  
13 Mikoviny, T., Riemer, D., Sachse, G. W., Sessions, W., Weber, R. J., Weinheimer, A. J.,  
14 Wisthaler, A., and Jimenez, J. L.: Effects of aging on organic aerosol from open biomass  
15 burning smoke in aircraft and laboratory studies, *Atmospheric Chemistry and Physics*, 11,  
16 12049-12064, 10.5194/acp-11-12049-2011, 2011.

17 de Gouw, J., and Warneke, C.: Measurements of volatile organic compounds in the earths  
18 atmosphere using proton-transfer-reaction mass spectrometry, *Mass Spectrometry Reviews*,  
19 26, 223-257, 10.1002/mas.20119, 2007.

20 Dunne, E., Galbally, I. E., Lawson, S. J., and Patti, A.: Interference in the PTR-MS  
21 measurement of acetonitrile at  $m/z$  42 in polluted urban air—A study using switchable  
22 reagent ion PTR-MS, *International Journal of Mass Spectrometry*, In press,  
23 10.1016/j.ijms.2012.05.004, 2012.

24 Engelhart, G. J., Hennigan, C. J., Miracolo, M. A., Robinson, A. L., and Pandis, S. N.: Cloud  
25 condensation nuclei activity of fresh primary and aged biomass burning aerosol, *Atmospheric*  
26 *Chemistry and Physics*, 12, 7285-7293, 10.5194/acp-12-7285-2012, 2012.

27 Ferek, R. J., Reid, J. S., Hobbs, P. V., Blake, D. R., and Liousse, C.: Emission factors of  
28 hydrocarbons, halocarbons, trace gases and particles from biomass burning in Brazil, *Journal*  
29 *of Geophysical Research: Atmospheres*, 103, 32107-32118, 10.1029/98JD00692, 1998.

30 Fletcher, C. A., Johnson, G. R., Ristovski, Z. D., and Harvey, M.: Hygroscopic and volatile  
31 properties of marine aerosol observed at Cape Grim during the P2P campaign, *Environmental*  
32 *Chemistry*, 4, 162-171, 10.1071/en07011, 2007.

33 Galbally, I. E., Lawson, S. J., Weeks, I. A., Bentley, S. T., Gillett, R. W., Meyer, M., and  
34 Goldstein, A. H.: Volatile organic compounds in marine air at Cape Grim, Australia,  
35 *Environmental Chemistry*, 4, 178-182, 10.1071/en07024, 2007.

36 Galbally, I. E., Meyer, C. P., Bentley, S. T., Lawson, S. J., and Baly, S. B.: Reactive gases in  
37 near surface air at Cape Grim, 2005-2006 Baseline Atmospheric Program (Australia), edited  
38 by: Cainey, J.M., Derek, N. and Krummel, P.B., Australian Bureau of Meteorology and  
39 CSIRO Marine and Atmospheric Research, 77-79, 2007b, available at:  
40 [http://www.bom.gov.au/inside/cgbaps/baseline/Baseline\\_2005-2006.pdf](http://www.bom.gov.au/inside/cgbaps/baseline/Baseline_2005-2006.pdf)

41 Gras, J. L.: Particles Program Report, 2005-2006 Baseline Atmospheric Program (Australia),  
42 edited by: Cainey, J.M., Derek, N. and Krummel, P.B., Australian Bureau of Meteorology  
43 and CSIRO Marine and Atmospheric Research, 85-86, 2007, available at:  
44 [http://www.bom.gov.au/inside/cgbaps/baseline/Baseline\\_2005-2006.pdf](http://www.bom.gov.au/inside/cgbaps/baseline/Baseline_2005-2006.pdf)

1 Hecobian, A., Liu, Z., Hennigan, C. J., Huey, L. G., Jimenez, J. L., Cubison, M. J., Vay, S.,  
2 Diskin, G. S., Sachse, G. W., Wisthaler, A., Mikoviny, T., Weinheimer, A. J., Liao, J.,  
3 Knapp, D. J., Wennberg, P. O., Kurten, A., Crouse, J. D., St Clair, J., Wang, Y., and Weber,  
4 R. J.: Comparison of chemical characteristics of 495 biomass burning plumes intercepted by  
5 the NASA DC-8 aircraft during the ARCTAS/CARB-2008 field campaign, *Atmospheric*  
6 *Chemistry and Physics*, 11, 13325-13337, 10.5194/acp-11-13325-2011, 2012.

7 Hennigan, C. J., Miracolo, M. A., Engelhart, G. J., May, A. A., Presto, A. A., Lee, T.,  
8 Sullivan, A. P., McMeeking, G. R., Coe, H., Wold, C. E., Hao, W. M., Gilman, J. B., Kuster,  
9 W. C., de Gouw, J., Schichtel, B. A., Collett, J. L., Kreidenweis, S. M., and Robinson, A. L.:  
10 Chemical and physical transformations of organic aerosol from the photo-oxidation of open  
11 biomass burning emissions in an environmental chamber, *Atmospheric Chemistry and*  
12 *Physics*, 11, 7669-7686, 10.5194/acp-11-7669-2011, 2011.

13 Hennigan, C. J., Westervelt, D. M., Riipinen, I., Engelhart, G. J., Lee, T., Collett, J. L.,  
14 Pandis, S. N., Adams, P. J., and Robinson, A. L.: New particle formation and growth in  
15 biomass burning plumes: An important source of cloud condensation nuclei, *Geophysical*  
16 *Research Letters*, 39, L09805, 10.1029/2012gl050930, 2012.

17 Hosseini, S., Urbanski, S. P., Dixit, P., Qi, L., Burling, I. R., Yokelson, R. J., Johnson, T. J.,  
18 Shrivastava, M., Jung, H. S., Weise, D. R., Miller, J. W., and Cocker, D. R.: Laboratory  
19 characterization of PM emissions from combustion of wildland biomass fuels, *Journal of*  
20 *Geophysical Research-Atmospheres*, 118, 9914-9929, 10.1002/jgrd.50481, 2013.

21 Hurst, D. F., Griffith, D. W. T., Carras, J. N., Williams, D. J., and Fraser, P. J.: Measurements  
22 of trace gases emitted by australian savanna fires during the 1990 dry season, *Journal of*  
23 *Atmospheric Chemistry*, 18, 33-56, 10.1007/bf00694373, 1994a.

24 Hurst, D. F., Griffith, D. W. T., and Cook, G. D.: Trace gas emissions from biomass burning  
25 in tropical australian savannas, *Journal of Geophysical Research-Atmospheres*, 99, 16441-  
26 16456, 10.1029/94jd00670, 1994b.

27 ISO: ISO 6879 Air Quality, Performance Characteristics and Related Concepts for Air  
28 Quality Measuring Methods, in, ISO, Geneva, 1995.

29 Inomata, S., Tanimoto, H., Kameyama, S., Tsunogai, U., Irie, H., Kanaya, Y., and Wang, Z.:  
30 Technical Note: Determination of formaldehyde mixing ratios in air with PTR-MS:  
31 laboratory experiments and field measurements, *Atmospheric Chemistry and Physics*, 8, 273-  
32 284, 2008.

33 Jaffe, D. A., and Wigder, N. L.: Ozone production from wildfires: A critical review,  
34 *Atmospheric Environment*, 51, 1-10, 10.1016/j.atmosenv.2011.11.063, 2012.

35 Janhäll, S., Andreae, M. O., and Pöschl, U.: Biomass burning aerosol emissions from  
36 vegetation fires: particle number and mass emission factors and size distributions, *Atmos.*  
37 *Chem. Phys.*, 10, 1427-1439, 10.5194/acp-10-1427-2010, 2010.

38 Karl, M., Gross, A., Leck, C., and Pirjola, L.: Intercomparison of dimethylsulfide oxidation  
39 mechanisms for the marine boundary layer: Gaseous and particulate sulfur constituents,  
40 *Journal of Geophysical Research-Atmospheres*, 112, D15304  
41 10.1029/2006jd007914, 2007a.

42 Karl, T. G., Christian, T. J., Yokelson, R. J., Artaxo, P., Hao, W. M., and Guenther, A.: The  
43 Tropical Forest and Fire Emissions Experiment: method evaluation of volatile organic  
44 compound emissions measured by PTR-MS, FTIR, and GC from tropical biomass burning,  
45 *Atmospheric Chemistry and Physics*, 7, 5883-5897, 2007b.

1 Keywood, M., Kanakidou, M., Stohl, A., Dentener, F., Grassi, G., Meyer, C. P., Torseth, K.,  
2 Edwards, D., Thompson, A., Lohmann, U., and Burrows, J. P.: Fire in the Air- Biomass  
3 burning impacts in a changing climate, *Critical Reviews in Environmental Science and*  
4 *Technology*, DOI:10.1080/10643389.2011.604248 2011.

5 Kitchener, A., and Harris, S.: From Forest to Fjaeldmark: Descriptions of Tasmania's  
6 Vegetation, 2 ed., Department of Primary Industries, Parks, Water and Environment,  
7 Tasmania, 2013.

8 Kondo, Y., Matsui, H., Moteki, N., Sahu, L., Takegawa, N., Kajino, M., Zhao, Y., Cubison,  
9 M. J., Jimenez, J. L., Vay, S., Diskin, G. S., Anderson, B., Wisthaler, A., Mikoviny, T.,  
10 Fuelberg, H. E., Blake, D. R., Huey, G., Weinheimer, A. J., Knapp, D. J., and Brune, W. H.:  
11 Emissions of black carbon, organic, and inorganic aerosols from biomass burning in North  
12 America and Asia in 2008, *Journal of Geophysical Research-Atmospheres*, 116,  
13 10.1029/2010jd015152, 2011.

14 Korhonen, H., Carslaw, K. S., Spracklen, D. V., Mann, G. W., and Woodhouse, M. T.:  
15 Influence of oceanic dimethyl sulfide emissions on cloud condensation nuclei concentrations  
16 and seasonality over the remote Southern Hemisphere oceans: A global model study, *Journal*  
17 *of Geophysical Research-Atmospheres*, 113, D15204 10.1029/2007jd009718, 2008.

18 Krummel, P. B., Fraser, P., Steele, L. P., Porter, L. W., Derek, N., Rickard, C., Dunse, B. L.,  
19 Langenfelds, R. L., Miller, B. R., Baly, S. B., and McEwan, S., The AGAGE in situ program  
20 for non-CO<sub>2</sub> greenhouse gases at Cape Grim, 2005-2006: methane, nitrous oxide, carbon  
21 monoxide, hydrogen, CFCs, HCFCs, HFCs, PFCs, halons, chlorocarbons, hydrocarbons and  
22 sulphur hexafluoride, 2005-2006 Baseline Atmospheric Program (Australia), edited by:  
23 Caine, J.M., Derek, N. and Krummel, P.B., Australian Bureau of Meteorology and CSIRO  
24 Marine and Atmospheric Research, 65-77, 2007, available at:  
25 [http://www.bom.gov.au/inside/cgbaps/baseline/Baseline\\_2005-2006.pdf](http://www.bom.gov.au/inside/cgbaps/baseline/Baseline_2005-2006.pdf)

26 Lawler, M. J., Whitehead, J., O'Dowd, C., Monahan, C., McFiggans, G., and Smith, J. N.:  
27 Composition of 15–85 nm particles in marine air, *Atmos. Chem. Phys.*, 14, 11557-11569,  
28 10.5194/acp-14-11557-2014, 2014.

29 Lawson, S. J., Cope, M., Lee, S., Keywood, M., Galbally, I. E., and Ristovski, Z.: Biomass  
30 Burning at Cape Grim: using modelling to explore plume photochemistry and composition,  
31 *Atmos. Chem. Phys.*, 2015. In preparation.

32 Lewis, A. C., Evans, M. J., Hopkins, J. R., Punjabi, S., Read, K. A., Purvis, R. M., Andrews,  
33 S. J., Moller, S. J., Carpenter, L. J., Lee, J. D., Rickard, A. R., Palmer, P. I., and Parrington,  
34 M.: The influence of biomass burning on the global distribution of selected non-methane  
35 organic compounds, *Atmospheric Chemistry and Physics*, 13, 851-867, 10.5194/acp-13-851-  
36 2013, 2013.

37 Martin, M., Tritscher, T., Jurányi, Z., Heringa, M. F., Sierau, B., Weingartner, E., Chirico, R.,  
38 Gysel, M., Prévôt, A. S. H., Baltensperger, U., and Lohmann, U.: Hygroscopic properties of  
39 fresh and aged wood burning particles, *J. Aerosol. Sci.*, 56, 15-29,  
40 <http://dx.doi.org/10.1016/j.jaerosci.2012.08.006>, 2013.

41 May, A. A., McMeeking, G. R., Lee, T., Taylor, J. W., Craven, J. S., Burling, I., Sullivan, A.  
42 P., Akagi, S., Collett, J. L., Flynn, M., Coe, H., Urbanski, S. P., Seinfeld, J. H., Yokelson, R.  
43 J., and Kreidenweis, S. M.: Aerosol emissions from prescribed fires in the United States: A  
44 synthesis of laboratory and aircraft measurements, *Journal of Geophysical Research:*  
45 *Atmospheres*, 119, 11,826-811,849, 10.1002/2014JD021848, 2014.

- 1 McCulloch, A., Midgley, P. M., and Ashford, P.: Releases of refrigerant gases (CFC-12,  
2 HCFC-22 and HFC-134a) to the atmosphere, *Atmospheric Environment*, 37, 889-902,  
3 [http://dx.doi.org/10.1016/S1352-2310\(02\)00975-5](http://dx.doi.org/10.1016/S1352-2310(02)00975-5), 2003.
- 4 McKenzie, L. M., Ward, D. E., and Hao, W. M.: Chlorine and bromine in the biomass of  
5 tropical and temperate ecosystems, *Biomass Burning and Global Change*, vol. 1, Remote  
6 Sensing, Modeling and Inventory Development, and Biomass Burning in Africa, edited by:  
7 J.S., L., MIT Press, Cambridge, Massachusetts, 1996.
- 8 Meyer, C. P., Cook, G. D., Reisen, F., Smith, T. E. L., Tattaris, M., Russell-Smith, J., Maier,  
9 S., Yates, C. P., and Wooster, M. J.: Direct measurements of the seasonality of emission  
10 factors from savanna fires in northern Australia, *Journal of Geophysical Research-*  
11 *Atmospheres*, 117, 2012.
- 12 Meyer, C. P., and Cook, G. D.: Biomass combustion and emission processes in the Northern  
13 Australian Savannas, in: *Carbon Accounting and Savanna Fire Management*, edited by:  
14 Murphy, B. P., Edwards, A. C., Meyer, C. P., and Russell-Smith, J., CSIRO Publishing,  
15 Clayton Australia 185-234 2015.
- 16 Miller, B. R., Weiss, R. F., Salameh, P. K., Tanhua, T., Grealley, B. R., Mühle, J., and  
17 Simmonds, P. G.: Medusa: A Sample Preconcentration and GC/MS Detector System for in  
18 Situ Measurements of Atmospheric Trace Halocarbons, Hydrocarbons, and Sulfur  
19 Compounds, *Anal. Chem.*, 80, 1536-1545, [10.1021/ac702084k](https://doi.org/10.1021/ac702084k), 2008.
- 20 Ortega, A. M., Day, D. A., Cubison, M. J., Brune, W. H., Bon, D., de Gouw, J. A., and  
21 Jimenez, J. L.: Secondary organic aerosol formation and primary organic aerosol oxidation  
22 from biomass-burning smoke in a flow reactor during FLAME-3, *Atmospheric Chemistry*  
23 *and Physics*, 13, 11551-11571, [10.5194/acp-13-11551-2013](https://doi.org/10.5194/acp-13-11551-2013), 2013.
- 24 Paton-Walsh, C., Jones, N. B., Wilson, S. R., Haverd, V., Meier, A., Griffith, D. W. T., and  
25 Rinsland, C. P.: Measurements of trace gas emissions from Australian forest fires and  
26 correlations with coincident measurements of aerosol optical depth, *Journal of Geophysical*  
27 *Research-Atmospheres*, 110, [10.1029/2005jd006202](https://doi.org/10.1029/2005jd006202), 2005.
- 28 Paton-Walsh, C., Wilson, S. R., Jones, N. B., and Griffith, D. W. T.: Measurement of  
29 methanol emissions from Australian wildfires by ground-based solar Fourier transform  
30 spectroscopy, *Geophysical Research Letters*, 35, 5, [L08810,10.1029/2007gl032951](https://doi.org/10.1029/2007gl032951), 2008.
- 31 Paton-Walsh, C., Deutscher, N. M., Griffith, D. W. T., Forgan, B. W., Wilson, S. R., Jones,  
32 N. B., and Edwards, D. P.: Trace gas emissions from savanna fires in northern Australia,  
33 *Journal of Geophysical Research-Atmospheres*, 115, 12, [D16314m 10.1029/2009jd013309](https://doi.org/10.1029/2009jd013309),  
34 2010.
- 35 Paton-Walsh, C., Emmons, L. K., and Wiedinmyer, C.: Australia's Black Saturday fires -  
36 comparison of techniques for estimating emissions from vegetation fires, *Atmospheric*  
37 *Environment*, 60, 262-270, [10.1016/j.atmosenv.2012.06.066](https://doi.org/10.1016/j.atmosenv.2012.06.066), 2012.
- 38 Paton-Walsh, C., Smith, T. E. L., Young, E. L., Griffith, D. W. T., and Guérette, É. A.: New  
39 emission factors for Australian vegetation fires measured using open-path Fourier transform  
40 infrared spectroscopy &ndash; Part 1: methods and Australian temperate forest fires, *Atmos.*  
41 *Chem. Phys. Discuss.*, 14, 4327-4381, [10.5194/acpd-14-4327-2014](https://doi.org/10.5194/acpd-14-4327-2014), 2014.
- 42 Petters, M. D., Carrico, C. M., Kreidenweis, S. M., Prenni, A. J., DeMott, P. J., Collett, J. L.,  
43 and Moosmüller, H.: Cloud condensation nucleation activity of biomass burning aerosol,  
44 *Journal of Geophysical Research: Atmospheres*, 114, n/a-n/a, [10.1029/2009JD012353](https://doi.org/10.1029/2009JD012353), 2009.

1 Pratt, K. A., Murphy, S. M., Subramanian, R., DeMott, P. J., Kok, G. L., Campos, T., Rogers,  
2 D. C., Prenni, A. J., Heymsfield, A. J., Seinfeld, J. H., and Prather, K. A.: Flight-based  
3 chemical characterization of biomass burning aerosols within two prescribed burn smoke  
4 plumes, *Atmospheric Chemistry and Physics*, 11, 12549-12565, 10.5194/acp-11-12549-2011,  
5 2011.

6 Prinn, R. G., Weiss, R. F., Fraser, P. J., Simmonds, P. G., Cunnold, D. M., Alyea, F. N.,  
7 O'Doherty, S., Salameh, P., Miller, B. R., Huang, J., Wang, R. H. J., Hartley, D. E., Harth, C.,  
8 Steele, L. P., Sturrock, G., Midgley, P. M., and McCulloch, A.: A history of chemically and  
9 radiatively important gases in air deduced from ALE/GAGE/AGAGE, *Journal of*  
10 *Geophysical Research: Atmospheres*, 105, 17751-17792, 10.1029/2000JD900141, 2000.

11 Quinn, P. K., and Bates, T. S.: The case against climate regulation via oceanic phytoplankton  
12 sulphur emissions, *Nature*, 480, 51-56, 10.1038/nature10580, 2011.

13 Reinhardt, T. E., and Ward, D. E.: Factors Affecting Methyl Chloride Emissions from Forest  
14 Biomass Combustion, *Environmental Science & Technology*, 29, 825-832,  
15 10.1021/es00003a034, 1995.

16 Sahu, L. K., Kondo, Y., Moteki, N., Takegawa, N., Zhao, Y., Cubison, M. J., Jimenez, J. L.,  
17 Vay, S., Diskin, G. S., Wisthaler, A., Mikoviny, T., Huey, L. G., Weinheimer, A. J., and  
18 Knapp, D. J.: Emission characteristics of black carbon in anthropogenic and biomass burning  
19 plumes over California during ARCTAS-CARB 2008, *Journal of Geophysical Research-*  
20 *Atmospheres*, 117, 10.1029/2011jd017401, 2012.

21 Shirai, T., Blake, D. R., Meinardi, S., Rowland, F. S., Russell-Smith, J., Edwards, A., Kondo,  
22 Y., Koike, M., Kita, K., Machida, T., Takegawa, N., Nishi, N., Kawakami, S., and Ogawa,  
23 T.: Emission estimates of selected volatile organic compounds from tropical savanna burning  
24 in northern Australia, *Journal of Geophysical Research-Atmospheres*, 108,  
25 10.1029/2001jd000841, 2003.

26 Simpson, I. J., Akagi, S. K., Barletta, B., Blake, N. J., Choi, Y., Diskin, G. S., Fried, A.,  
27 Fuelberg, H. E., Meinardi, S., Rowland, F. S., Vay, S. A., Weinheimer, A. J., Wennberg, P.  
28 O., Wiebring, P., Wisthaler, A., Yang, M., Yokelson, R. J., and Blake, D. R.: Boreal forest  
29 fire emissions in fresh Canadian smoke plumes: C(1)-C(10) volatile organic compounds  
30 (VOCs), CO(2), CO, NO(2), NO, HCN and CH(3)CN, *Atmospheric Chemistry and Physics*,  
31 11, 6445-6463, 10.5194/acp-11-6445-2011, 2011.

32 Smith, T. E. L., Paton-Walsh, C., Meyer, C. P., Cook, G. D., Maier, S. W., Russell-Smith, J.,  
33 Wooster, M. J., and Yates, C. P.: New emission factors for Australian vegetation fires  
34 measured using open-path Fourier transform infrared spectroscopy &ndash; Part 2:  
35 Australian tropical savanna fires, *Atmos. Chem. Phys. Discuss.*, 14, 6311-6360,  
36 10.5194/acpd-14-6311-2014, 2014.

37 Steele, L. P., Krummel, P. B., Spencer, D. A., Rickard, C., Baly, S. B., Langenfelds, R. L.,  
38 and van der Schoot, M. V., <http://www.bom.gov.au/inside/cgbaps/baseline.shtml> Baseline  
39 carbon dioxide monitoring, in: *Baseline Atmospheric Program Australia 2005-2006*, Baseline  
40 Atmospheric Program Australia 2005-2006, 2007.

41 Stockwell, C. E., Yokelson, R. J., Kreidenweis, S. M., Robinson, A. L., DeMott, P. J.,  
42 Sullivan, R. C., Reardon, J., Ryan, K. C., Griffith, D. W. T., and Stevens, L.: Trace gas  
43 emissions from combustion of peat, crop residue, domestic biofuels, grasses, and other fuels:  
44 configuration and Fourier transform infrared (FTIR) component of the fourth Fire Lab at  
45 Missoula Experiment (FLAME-4), *Atmospheric Chemistry and Physics*, 14, 9727-9754,  
46 10.5194/acp-14-9727-2014, 2014.

1 Stockwell, C. E., Veres, P. R., Williams, J., and Yokelson, R. J.: Characterization of biomass  
2 burning emissions from cooking fires, peat, crop residue, and other fuels with high-resolution  
3 proton-transfer-reaction time-of-flight mass spectrometry, *Atmos. Chem. Phys.*, 15, 845-865,  
4 10.5194/acp-15-845-2015, 2015.

5 Vakkari, V., Kerminen, V.-M., Beukes, J. P., Tiitta, P., van Zyl, P. G., Josipovic, M., Venter,  
6 A. D., Jaars, K., Worsnop, D. R., Kulmala, M., and Laakso, L.: Rapid changes in biomass  
7 burning aerosols by atmospheric oxidation, *Geophysical Research Letters*, 41,  
8 2014GL059396, 10.1002/2014GL059396, 2014.

9 van Leeuwen, T. T., and van der Werf, G. R.: Spatial and temporal variability in the ratio of  
10 trace gases emitted from biomass burning, *Atmospheric Chemistry and Physics*, 11, 3611-  
11 3629, 10.5194/acp-11-3611-2011, 2011.

12 Volkova, L., Meyer, C. P., Murphy, S., Fairman, T., Reisen, F., and Weston, C.: Fuel  
13 reduction burning mitigates wildfire effects on forest carbon and greenhouse gas emission,  
14 *International Journal of Wildland Fire*, 23, 771-780, <http://dx.doi.org/10.1071/WF14009>,  
15 2014.

16 Vollmer, M. K., Walter, S., Mohn, J., Steinbacher, M., Bond, S. W., Röckmann, T., and  
17 Reimann, S.: Molecular hydrogen (H<sub>2</sub>) combustion emissions and their isotope (D/H)  
18 signatures from domestic heaters, diesel vehicle engines, waste incinerator plants, and  
19 biomass burning, *Atmos. Chem. Phys.*, 12, 6275-6289, 10.5194/acp-12-6275-2012, 2012.

20 Ward, D. E., and Radke, L. F.: Emission measurements from vegetation fires: A comparative  
21 evaluation of methods and results, in: *Fire in the Environment: The Ecological, Atmospheric,  
22 and Climatic Importance of Vegetation Fires* John Wiley & Sons Ltd., 1993

23 Watson, J. G., Chow, J. C., Chen, L. W. A., Lowenthal, D. H., Fujita, E. M., Kuhns, H. D.,  
24 Sodeman, D. A., Campbell, D. E., Moosmüller, H., Zhu, D., and Motallebi, N.: Particulate  
25 emission factors for mobile fossil fuel and biomass combustion sources, *Sci. Total Environ.*,  
26 409, 2384-2396, <http://dx.doi.org/10.1016/j.scitotenv.2011.02.041>, 2011.

27 Wigder, N. L., Jaffe, D. A., and Saketa, F. A.: Ozone and particulate matter enhancements  
28 from regional wildfires observed at Mount Bachelor during 2004-2011, *Atmospheric  
29 Environment*, 75, 24-31, 10.1016/j.atmosenv.2013.04.026, 2013.

30 Yokelson, R. J., Goode, J. G., Ward, D. E., Susott, R. A., Babbitt, R. E., Wade, D. D.,  
31 Bertschi, I., Griffith, D. W. T., and Hao, W. M.: Emissions of formaldehyde, acetic acid,  
32 methanol, and other trace gases from biomass fires in North Carolina measured by airborne  
33 Fourier transform infrared spectroscopy, *Journal of Geophysical Research-Atmospheres*, 104,  
34 30109-30125, 10.1029/1999jd900817, 1999.

35 Yokelson, R. J., Bertschi, I. T., Christian, T. J., Hobbs, P. V., Ward, D. E., and Hao, W. M.:  
36 Trace gas measurements in nascent, aged, and cloud-processed smoke from African savanna  
37 fires by airborne Fourier transform infrared spectroscopy (AFTIR), *Journal of Geophysical  
38 Research-Atmospheres*, 108, 8478 10.1029/2002jd002322, 2003.

39 Yokelson, R. J., Urbanski, S. P., Atlas, E. L., Toohey, D. W., Alvarado, E. C., Crouse, J. D.,  
40 Wennberg, P. O., Fisher, M. E., Wold, C. E., Campos, T. L., Adachi, K., Buseck, P. R., and  
41 Hao, W. M.: Emissions from forest fires near Mexico City, *Atmos. Chem. Phys.*, 7, 5569-  
42 5584, 10.5194/acp-7-5569-2007, 2007. Yokelson, R. J., Crouse, J. D., DeCarlo, P. F., Karl,  
43 T., Urbanski, S., Atlas, E., Campos, T., Shinozuka, Y., Kapustin, V., Clarke, A. D.,  
44 Weinheimer, A., Knapp, D. J., Montzka, D. D., Holloway, J., Weibring, P., Flocke, F.,  
45 Zheng, W., Toohey, D., Wennberg, P. O., Wiedinmyer, C., Mauldin, L., Fried, A., Richter,  
46 D., Walega, J., Jimenez, J. L., Adachi, K., Buseck, P. R., Hall, S. R., and Shetter, R.:

- 1 Emissions from biomass burning in the Yucatan, *Atmospheric Chemistry and Physics*, 9,  
2 5785-5812, 2009.
- 3 Yokelson, R. J., Burling, I. R., Gilman, J. B., Warneke, C., Stockwell, C. E., de Gouw, J.,  
4 Akagi, S. K., Urbanski, S. P., Veres, P., Roberts, J. M., Kuster, W. C., Reardon, J., Griffith,  
5 D. W. T., Johnson, T. J., Hosseini, S., Miller, J. W., Cocker, D. R., Jung, H., and Weise, D.  
6 R.: Coupling field and laboratory measurements to estimate the emission factors of identified  
7 and unidentified trace gases for prescribed fires, *Atmospheric Chemistry and Physics*, 13, 89-  
8 116, 10.5194/acp-13-89-2013, 2013.

## 1 Tab01

Measurement	Instrument	Air intake height	Time resolution	Reference
NMOCs	PTR-MS	10m	10 min	(Galbally et al., 2007a)
Particle size distribution and number 14-700 nm	SMPS	10m	1 min	(Cravigan et al., 2015)
Condensation nuclei (particle number > 3 nm)	TSI particle counters	10m	1 min	(Gras, 2007)
black carbon concentration	aethelometer	10m	integrated 30 min	(Gras, 2007)
CCN number at 0.5% SS	CCN counter	10m	1 min	(Gras, 2007)
ozone (O <sub>3</sub> )	TECO analyser	10m	1 min	(Galbally et al., 2007b)
methane (CH <sub>4</sub> )	AGAGE GC-FID	10m/70m/75m	40 min (discrete air sample every 40 minutes)	(Prinn et al., 2000; Krummel et al., 2007)
carbon monoxide (CO) and hydrogen (H <sub>2</sub> )	AGAGE GC-MRD	10m/70m/75m	40 min (discrete air sample every 40 minutes)	(Prinn et al., 2000; Krummel et al., 2007)
carbon dioxide (CO <sub>2</sub> )	CSIRO LoFlo NDIR	70m	1 min (continuous analyser)	(Steele et al., 2007)
nitrous oxide (N <sub>2</sub> O), major CFCs, CHCl <sub>3</sub> , CH <sub>3</sub> CCl <sub>3</sub> , CCl <sub>4</sub>	AGAGE GC-ECD system	10m/70m/75m	40 min (discrete air sample every 40 minutes)	(Prinn et al., 2000; Krummel et al., 2007)
minor CFCs, HCFCs, HFCs, PFCs, methylhalides, chlorinated solvents, halons, ethane	AGAGE GC-MS-Medusa	75m	2 hour (20 minute integrated air sample every 2 hours)	(Miller et al., 2008; Prinn et al., 2000; Krummel et al., 2007)

1

2 Tab02

Event	Date and Time	Period	Air Mass Origin	Marker Species	Comments
BB 1	16/02/2006 2:00	A	Ocean & NW Tasmania	CO, BC, low O <sub>3</sub> , particles (uni modal)	Fresh Plume
	16/02/2006 6:00	B	Ocean & NW Tasmania	BC, O <sub>3</sub> , particle growth	Particle growth
	16/02/2006 12:00	C	mainland Australia	O <sub>3</sub> (overnight enhancement)	Background terrestrial
	17/02/2006 6:00	D	Melbourne	O <sub>3</sub> , particles, HFC-134a	Urban
	17/02/2006 15:00	E	Ocean	Particles (bi-modal)	Clean Marine
	18/02/2006 0:00	F	Ocean & mainland Australia	O <sub>3</sub> , HFC-134a	Marine with minor terrestrial
BB2	23/02/2006 23:00	A	Ocean & NW Tasmania	CO, BC, Acetonitrile, particles	Fresh Plume
	24/02/2006 23:00	B	mainland Australia	CO, NMOC (Acetonitrile)	Fresh plume + precipitation
	25/02/2006 5:00	C	Melbourne	HFC-134a, O <sub>3</sub>	Urban
	25/02/2006 23:00	D	Ocean	Low particles, HFC-134a	Clean Marine

Compound	formula	Background concentration <sup>a</sup>	BB plume concentration <sup>a</sup>	ER CO <sup>b</sup>	CO ER R <sup>2</sup>	EF (g kg <sup>-1</sup> ) <sup>c</sup>
<b>Species statistically enhanced in plume</b>		mean (stdev)	mean (stdev)			
carbon dioxide	CO <sub>2</sub>	378.1 (0.7)	382.9 (1.2)	1620	0.15	1621
carbon monoxide	CO	42 (6)	618 (279)	n/a	n/a	127
methane	CH <sub>4</sub>	1713 (2)	1743 (10)	49	0.48	3.8
nitrous oxide	N <sub>2</sub> O	319.0 (0.2)	319.1 (0.2)	0.27	0.01	0.06
hydrogen	H <sub>2</sub>	551 (3)	6010 (28)	100	0.87	0.93
ethane	C <sub>2</sub> H <sub>6</sub>	1845 (146)	1765 (1008)	3.2	0.79	0.41
hydrogen cyanide (m/z 28)	HCN	122 (4)	903 (292)	5.7	0.42	0.73
formaldehyde (m/z 31)	HCHO	541 (339)	1895 (561)	11	0.08	1.64
methanol (m/z 33)	CH <sub>3</sub> OH	721 (413)	8603 (2521)	14	0.43	2.07
acetonitrile (m/z 42)	C <sub>2</sub> H <sub>3</sub> N	35 (4)	983 (324)	1.3	0.58	0.25
acetaldehyde (m/z 45)	CH <sub>3</sub> CHO	48 (27)	2608 (807)	4.4	0.53	0.92
unknown (m/z 46)	unknown	105 (72)	279 (74)	0.27	-0.9	0.06
formic acid (m/z 47)	CH <sub>2</sub> O <sub>2</sub>	19 (7)	141 (63)	0.20	-0.09	0.05
acetone/propanal (m/z 59)	C <sub>3</sub> H <sub>6</sub> O	170 (31)	1315 (372)	2.0	0.40	0.54
acetic acid (m/z 61)	CH <sub>3</sub> COOH	75 (32)	2054 (971)	3.6	0.64	0.75

furan/isoprene (m/z 69)	C <sub>4</sub> H <sub>4</sub> O	78 (39)	3113 (1139)	5.3	0.72	1.69
MVK/MAK (m/z 71)	C <sub>4</sub> H <sub>6</sub> O	14 (10)	673 (234)	1.2	0.76	0.38
methylglyoxal/methyl ethyl ketone (m/z 73)	C <sub>4</sub> H <sub>8</sub> O	21 (12)	618 (209)	1.0	0.69	0.35
benzene (m/z 79)	C <sub>6</sub> H <sub>6</sub>	7 (6)	1093 (390)	1.9	0.78	0.69
2-furanone (m/z 85)	C <sub>4</sub> H <sub>4</sub> O <sub>2</sub>	15 (5)	847 (276)	1.5	0.51	0.57
2,3-butanedione (m/z 87)	C <sub>4</sub> H <sub>6</sub> O <sub>2</sub>	16 (5)	576 (186)	0.97	0.67	0.39
toluene (m/z 93)	C <sub>7</sub> H <sub>8</sub>	8 (5)	409 (113)	0.69	0.51	0.30
phenol (m/z 95)	C <sub>6</sub> H <sub>5</sub> OH	12 (9)	472 (149)	0.80	0.73	0.35
unknown (m/z 101)	Unknown	15 (4)	124 (33)	0.19	0.32	0.09
xylenes (m/z 107)	C <sub>8</sub> H <sub>10</sub>	15 (0)	319 (100)	0.53	0.70	0.26
unknown (m/z 113)	unknown	9 (0)	279 (87)	0.47	0.60	0.25
C <sub>3</sub> -benzenes (m/z 121)	C <sub>9</sub> H <sub>12</sub>	20 (12)	290 (89)	0.47	0.73	0.27
monoterpenes + unknowns (m/z 137)	C <sub>10</sub> H <sub>16</sub> /C <sub>8</sub> H <sub>8</sub> O <sub>2</sub>	17 (9)	219 (79)	0.18	0.51	0.11
unknown (m/z 153)	unknown	45 (135)	91 (29)	0.09	0.61	0.06
methyl chloride	CH <sub>3</sub> Cl	594 (79)	1251 (458)	1.30	0.74	0.28
methyl bromide	CH <sub>3</sub> Br	9 (2)	34 (18)	0.05	0.74	0.02
methyl iodide	CH <sub>3</sub> I	1.3 (0.2)	3.7 (1.5)	0.004	0.75	0.002
black carbon	n/a	1.6 (0.3)	1657 (769)	0.003	0.81	0.16
CN > 3 nm	n/a	625 (2078)	24902 (8031)	38.4	0.7	n/a

CCN 0.5%	n/a	160 (31)	5501 (1355)	8.3	-0.4	n/a
<b>Species not statistically enhanced in plume</b>						
dimethyl sulphide (m/z 63)	C <sub>2</sub> H <sub>6</sub> S	158 (57)	172 (15)	n/a	n/a	n/a
chloroform	CHCl <sub>3</sub>	6.6 (0.5)	8.8 (1.4)	n/a	n/a	n/a
methyl chloroform	CH <sub>3</sub> CCl <sub>3</sub>	16.1 (0.2)	16.0 (0.2)	n/a	n/a	n/a
dichloromethane	CH <sub>2</sub> Cl <sub>2</sub>	7.5 (0.04)	7.6 (0.1)	n/a	n/a	n/a
carbon tetrachloride	CCl <sub>4</sub>	90.2 (0.7)	90.3 (0.2)	n/a	n/a	n/a
bromoform	CHBr <sub>3</sub>	4.2 (0.8)	4.7 (0.4)	n/a	n/a	n/a
HFC-32	CH <sub>2</sub> F <sub>2</sub>	1.02 (0.03)	1.04 (0.03)	n/a	n/a	n/a
HFC-125	C <sub>2</sub> HF <sub>5</sub>	3.57 (0.04)	3.63 (0.05)	n/a	n/a	n/a
HFC-134a	CH <sub>2</sub> FCF <sub>3</sub>	33.20 (0.22)	33.28 (0.17)	n/a	n/a	n/a
ozone	O <sub>3</sub>	15.1 (1.1)	15.8 (1.5)	n/a	n/a	n/a

1

2

## 1 Tab04

	This study g kg <sup>-1</sup> (coastal heath)	Temperate south eastern Australia	Tropical savannah Australia	Temperate Northern Hemisphere
Hydrogen (H <sub>2</sub> )	0.93	n/a	n/a	2.03 (1.79) <sup>j</sup>
Methane (CH <sub>4</sub> )	3.8	3.5 (1.1) <sup>c</sup>	2.26 (1.27) <sup>d</sup> 2.33 (0.80) <sup>e</sup> 2.20 (0.32) <sup>f</sup> 2.03 (0.13) <sup>h</sup> 2.10 (1.16) <sup>i</sup>	3.92 (2.39) <sup>j</sup> 3.69 (1.36) <sup>l</sup>
Ethane (C <sub>2</sub> H <sub>6</sub> )	0.41	0.26 (0.11) <sup>a</sup> 0.5 (0.2) <sup>c</sup>	0.60 (0.225) <sup>d</sup> 0.11 (0.09) <sup>e</sup> 0.53 (0.02) <sup>f</sup> 0.13 (0.04) <sup>g</sup> 0.08 (0.05) <sup>i</sup>	1.12 (0.67) <sup>j</sup> 0.48 (0.61) <sup>l</sup>
Hydrogen cyanide (HCN)	0.73	0.43 (0.22) <sup>a</sup>	0.036 (0.002) <sup>d</sup> 0.025 (0.024) <sup>e</sup> 0.11 (0.04) <sup>g</sup> 0.53 (0.31) <sup>i</sup>	0.73 (0.19) <sup>j</sup> 0.75 (0.26) <sup>l</sup>
Acetonitrile (CH <sub>3</sub> CN)	0.25	n/a	0.11 (0.06) <sup>f</sup>	0.15 (0.07) <sup>l</sup>
Acetaldehyde (C <sub>2</sub> H <sub>4</sub> O)	0.92	n/a	0.55 (0.26) <sup>d</sup> 1.0 (0.62) <sup>e</sup>	0.56 (0.40) <sup>l</sup>
Phenol (C <sub>6</sub> H <sub>5</sub> OH)	0.35	n/a	n/a	0.33 (0.38) <sup>j</sup>

1

					0.45 (0.19) <sup>i</sup>
Acetic acid (CH <sub>3</sub> COOH)	0.75	3.8 (1.3) <sup>c</sup>		1.54 (0.64) <sup>i</sup>	1.97 (1.66) <sup>j</sup> 1.91 (0.93) <sup>i</sup>
Methanol (CH <sub>3</sub> OH)	2.07	2.3 (0.8) <sup>b</sup> 2.4 (1.2) <sup>c</sup>		1.06 (0.87) <sup>i</sup>	1.93 (1.38) <sup>j</sup> 1.35 (0.4) <sup>i</sup>
Benzene (C <sub>6</sub> H <sub>6</sub> )	0.69	n/a		0.42 (0.23) <sup>d</sup> 0.29 (0.24) <sup>e</sup> 0.21 (0.02) <sup>f</sup>	0.45 (0.29) <sup>i</sup>
Toluene (C <sub>7</sub> H <sub>8</sub> )	0.30	n/a		n/a	0.17 (0.13) <sup>i</sup>
Methyl chloride (CH <sub>3</sub> Cl)	0.28	n/a		0.0605 (0.0072) <sup>f</sup>	0.059 <sup>k</sup>
Methyl bromide (CH <sub>3</sub> Br)	0.02	n/a		0.0018 (0.0003) <sup>f</sup>	0.0036 <sup>k</sup>
Methyl iodide(CH <sub>3</sub> I)	0.002	n/a		n/a	0.0008 <sup>k</sup>

1 Table 1. Measurement summary

2 Table 2. Summary of Periods described in the text for BB1 and BB2 (as shown in Figs 3 and  
3 6)

4 Table 3. Summary of species measured in BB2 coastal heathland fire including background  
5 concentration, plume concentration, ER to CO and EF. <sup>a</sup> Units – all in ppt except for CO,  
6 CH<sub>4</sub>, N<sub>2</sub>O in ppb, CO<sub>2</sub> in ppm, CN and CCN in particles cm<sup>-3</sup>, BC in ng m<sup>-3</sup> <sup>b</sup>Trace gas  
7 emission ratios are molar ratios, BC is mass ratio, particle number is # particles ppb<sup>-1</sup> <sup>c</sup>  
8 calculated using carbon mass balance method n/a = not applicable

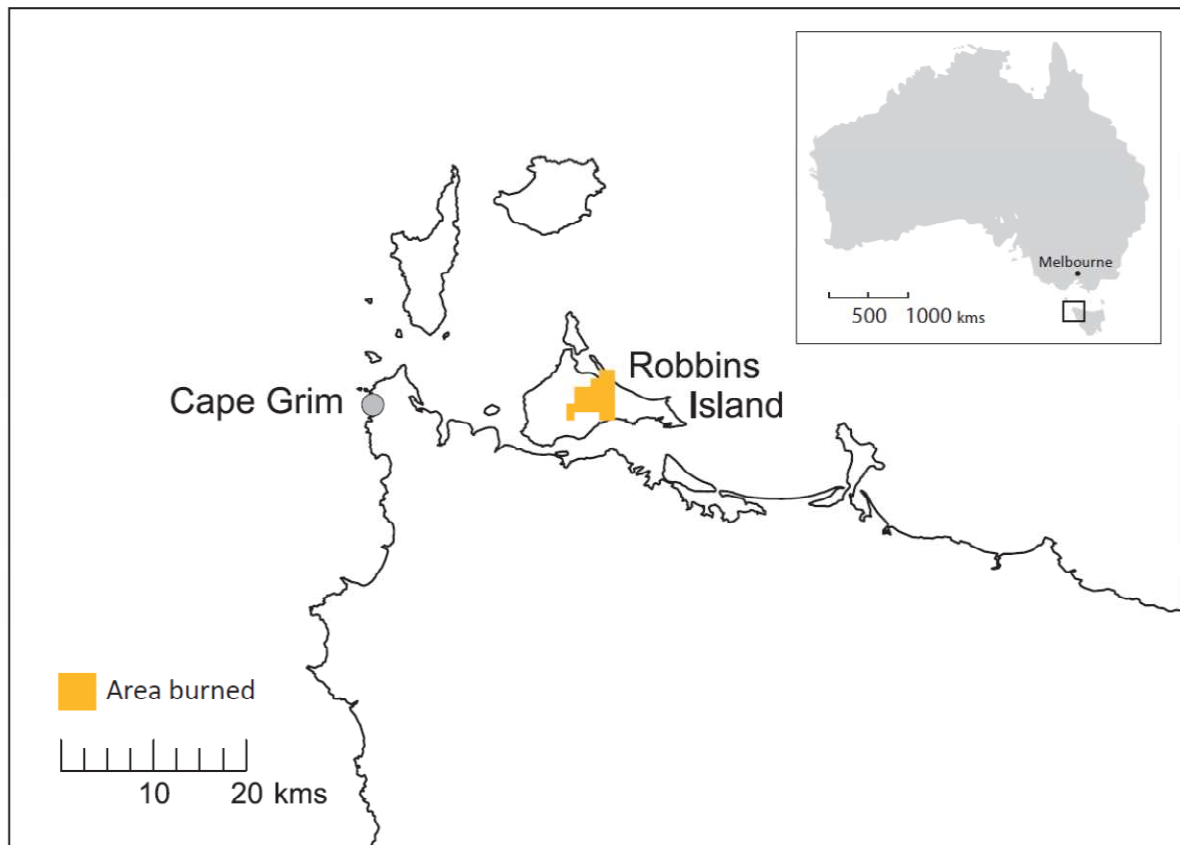
9 Table 4. Comparison of emission factors with other studies

10 <sup>a</sup> Paton-Walsh et al., 2005, <sup>b</sup> Paton-Walsh et al., 2008, <sup>c</sup> Paton-Walsh et al., 2014, <sup>d</sup>Hurst et  
11 al., 1994a <sup>e</sup>Hurst et al., 1994b <sup>f</sup> Shirai et al., 2003 <sup>g</sup> Paton-Walsh et al., 2010 <sup>h</sup> Meyer et al.,  
12 2012 <sup>i</sup> Smith et al., 2014 <sup>j</sup>Akagi et al., 2011 temperate updated May 2014 <sup>k</sup>Akagi et al., 2011  
13 extratropical <sup>l</sup>Yokelson et al., 2013 semi arid shrubland

14

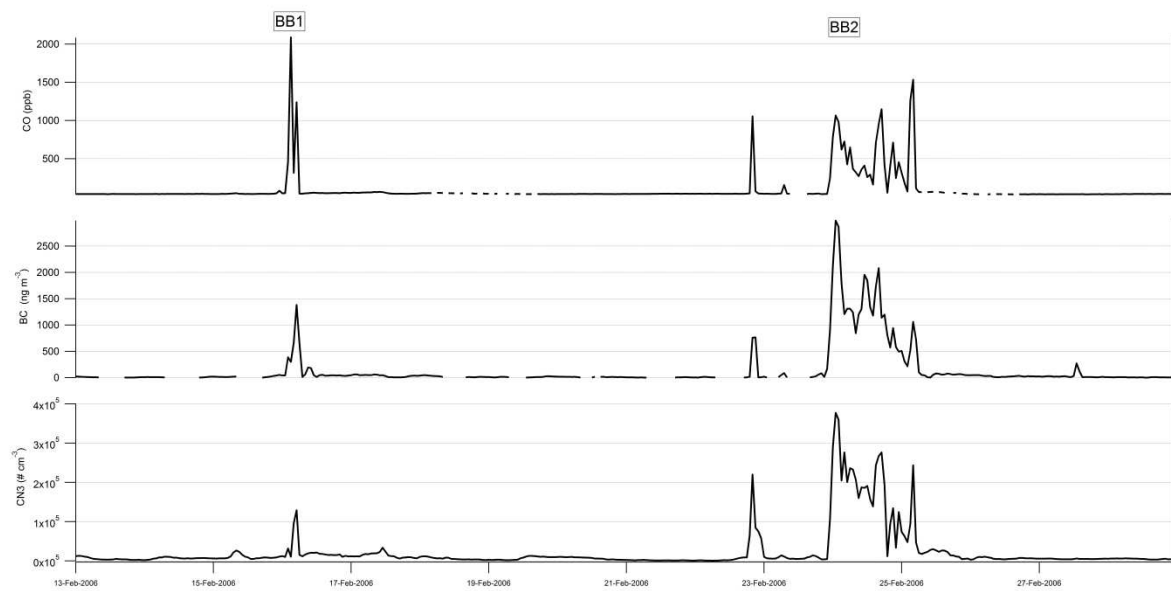
15

1 Fig 01



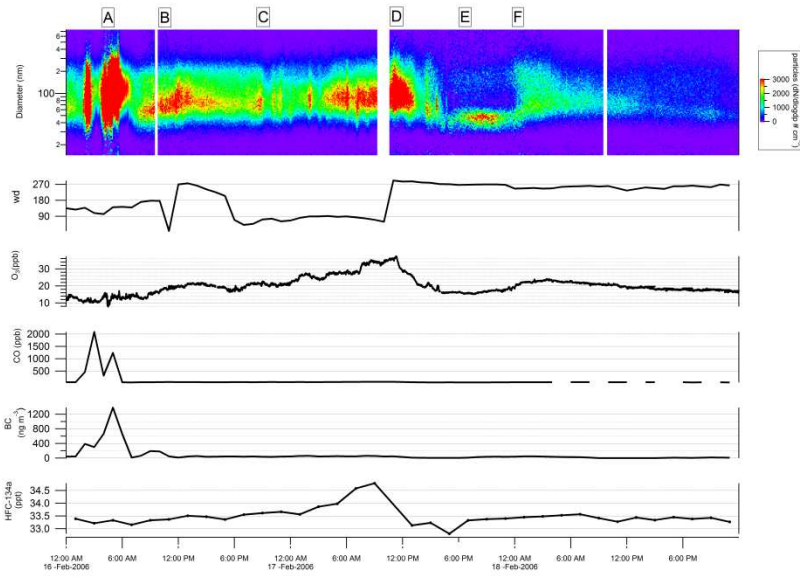
2

3 Fig 02



4

5 Fig 03



1

2 Fig 04

3

4

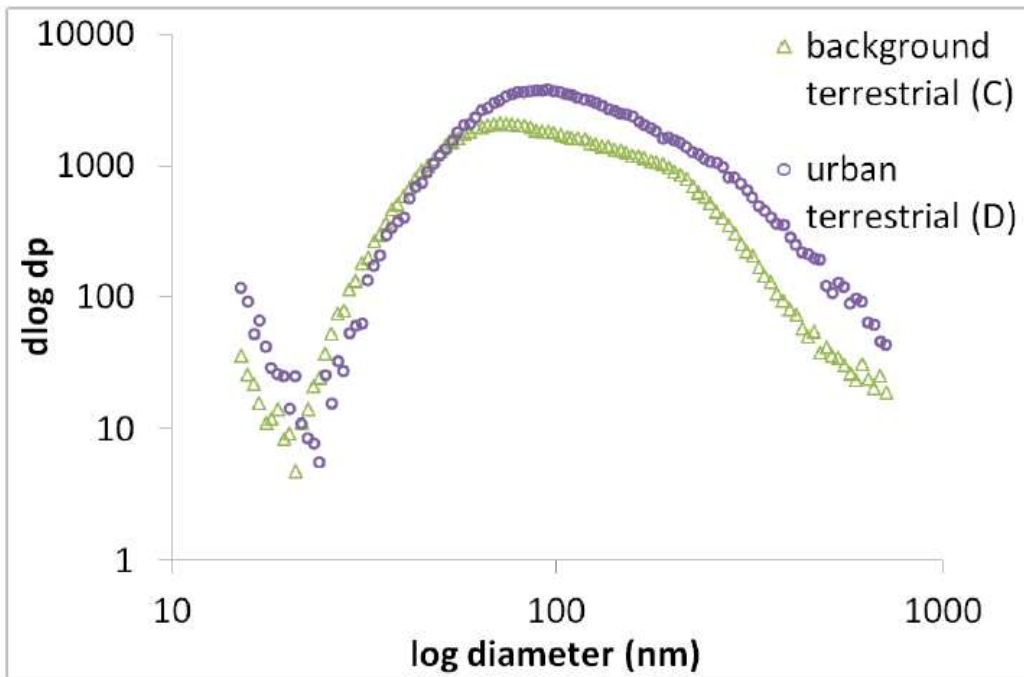


Fig04b

5

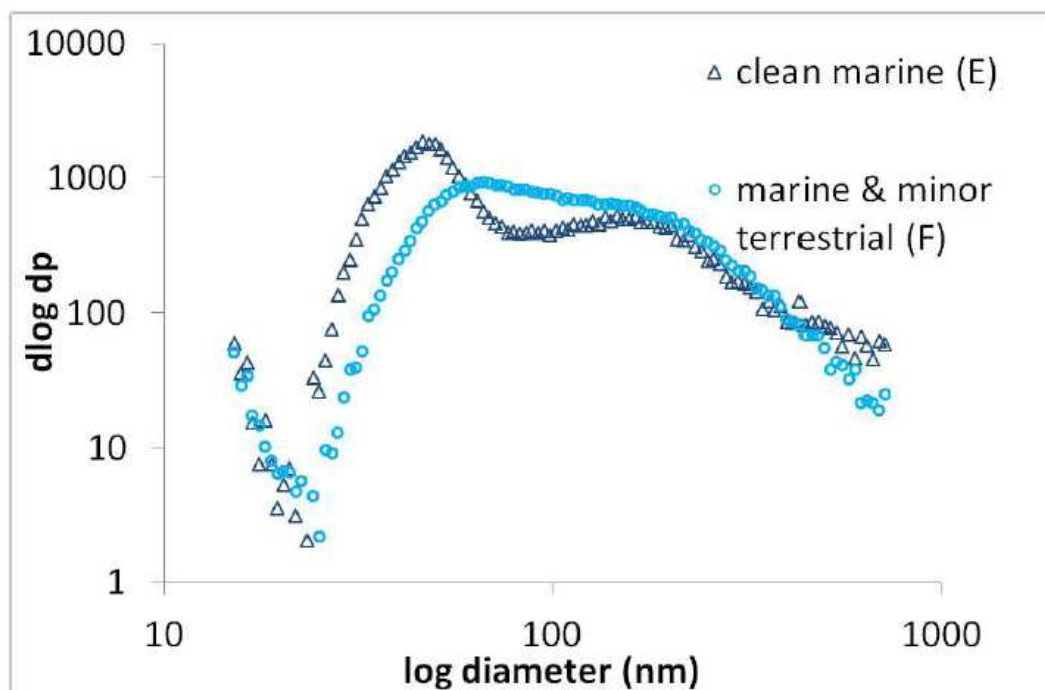


Fig 04c

1

2 Fig 05

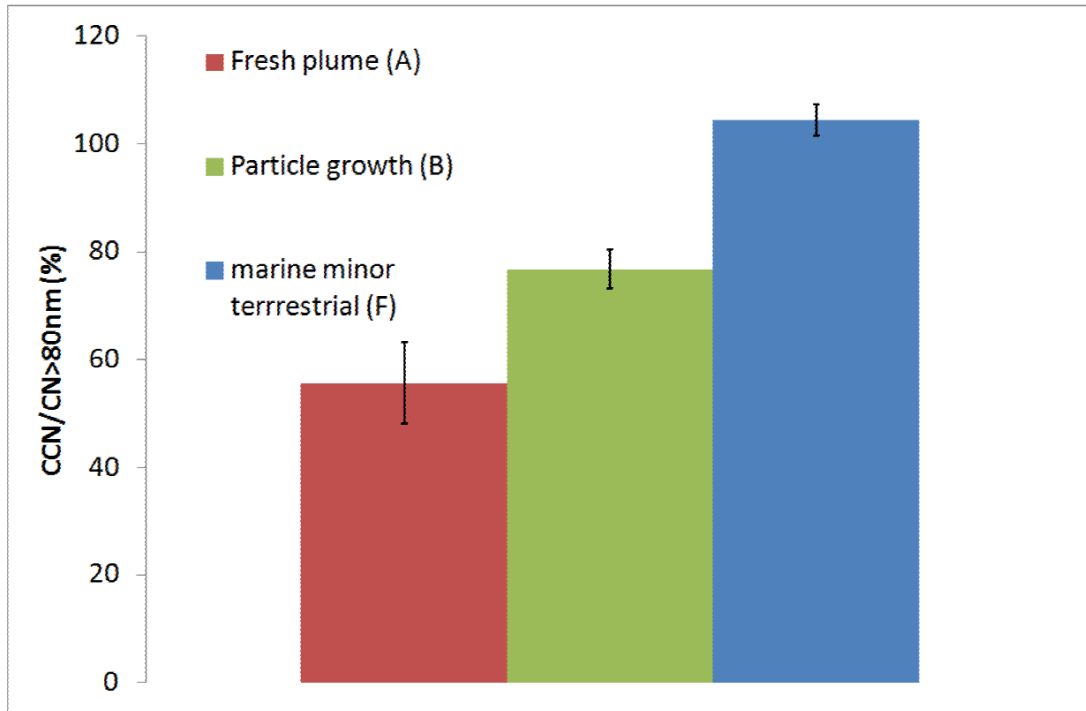


Fig05a

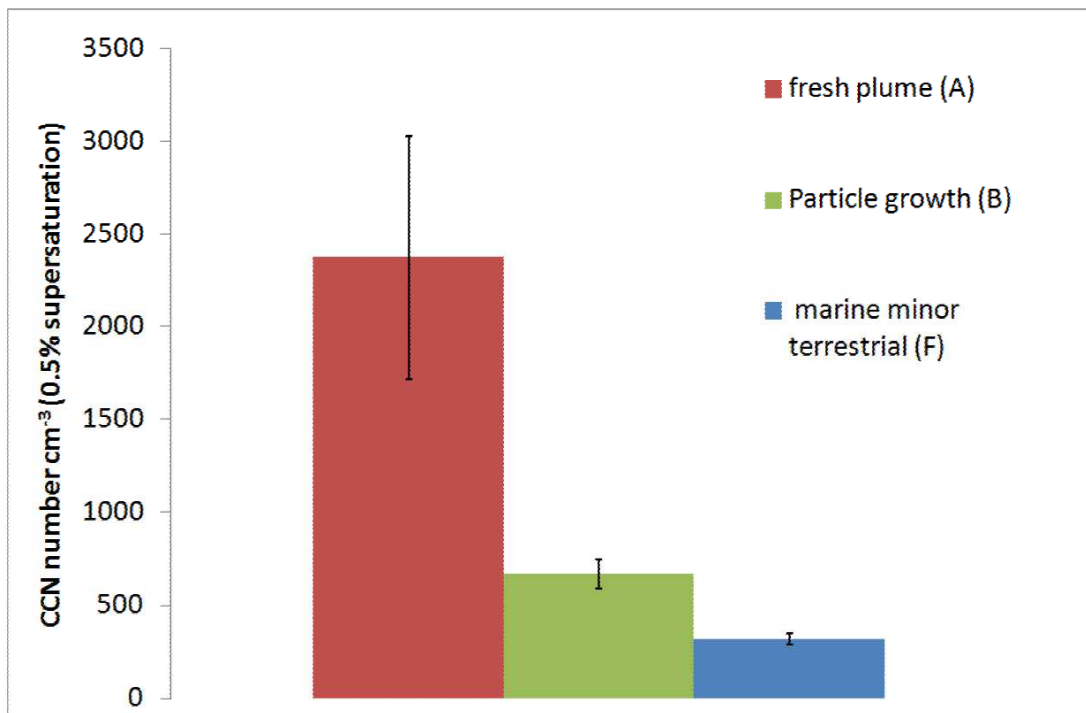
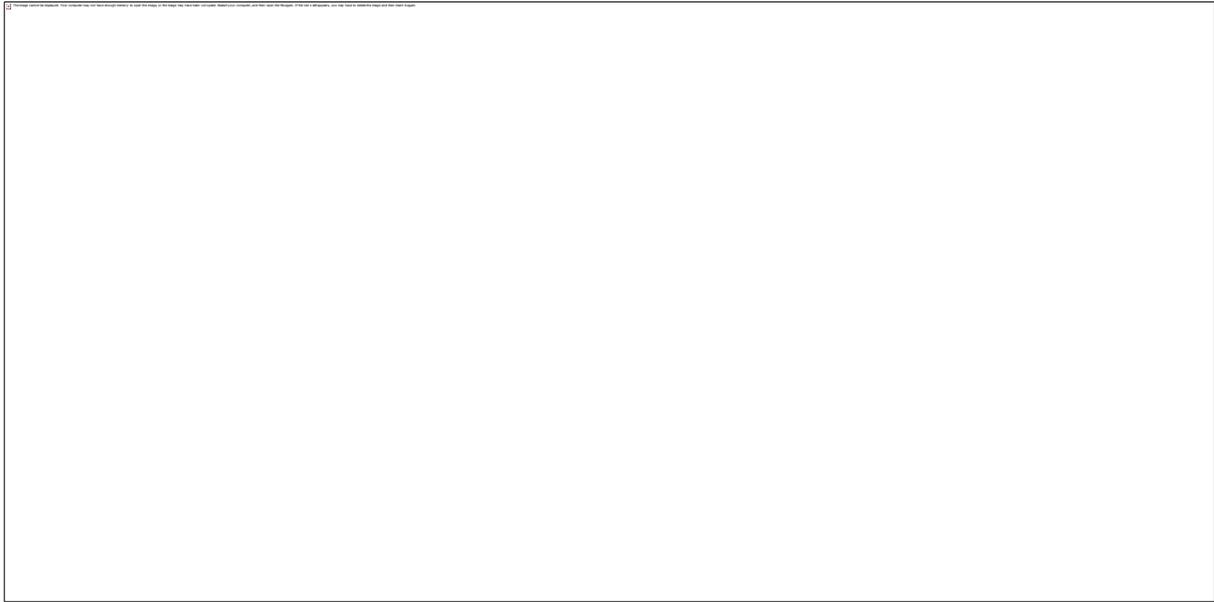


Fig05b

1

2

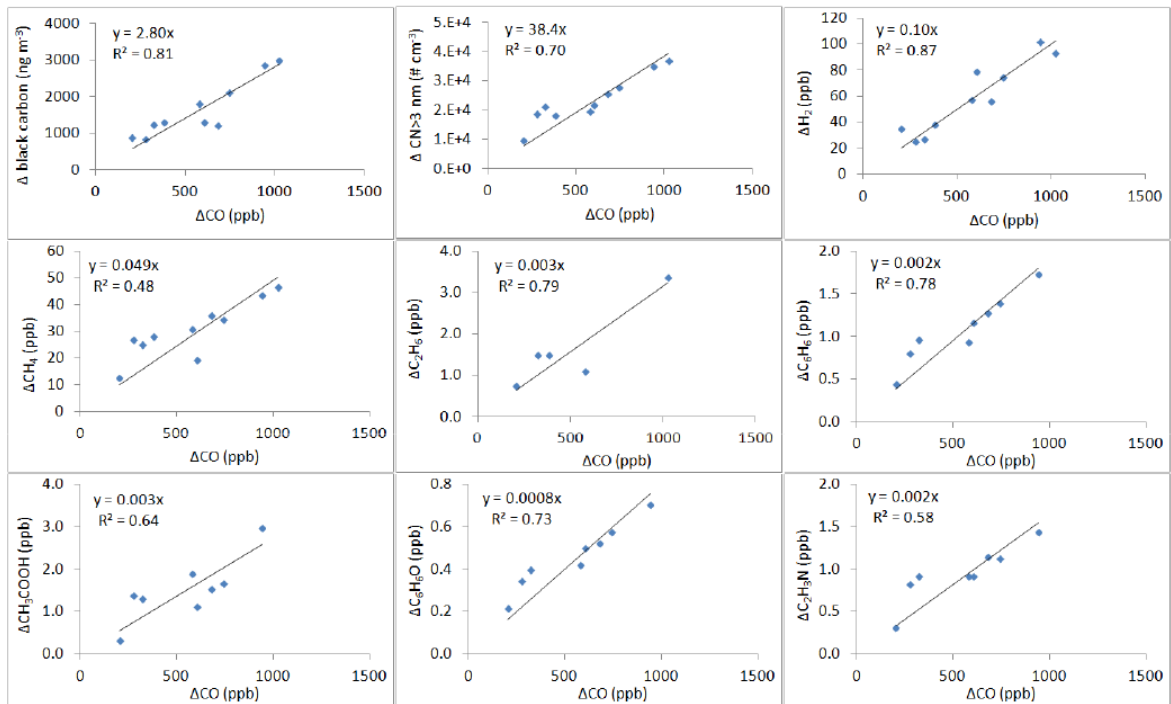
3 Fig 06



1

2

3 Fig 07



4

5

6 Figure 1. Location of Cape Grim and Robbins Island in North West Tasmania, Australia.

7 Area burned is shown.

1 Figure 2. Time series of carbon monoxide (CO), black carbon (BC) and particles $>3$  nm  
2 (CN<sub>3</sub>) for the study period (BB 1 and BB2 shown).

3 Figure 3. Time series from BB1 including a particle size and number contour plot, wind  
4 direction (degrees), ozone (O<sub>3</sub>), carbon monoxide (CO), black carbon (BC) and HFC-134a.  
5 Periods A-F are discussed in the text.

6 Figure 4. Average particle size distributions (with log scale on both axes) from BB1  
7 corresponding to periods shown in Fig 3 including (a) the fresh plume (Period A) and particle  
8 growth (Period B) (b) background terrestrial (Period C) and urban terrestrial (Period D) and  
9 (c) clean marine (Period E) and marine and minor terrestrial (Period F).

10 Figure 5 (a) Average ratios of CCN/CN $>80$  (hourly) in BB1 during fresh plume (Fig 3.  
11 Period A), particle growth event (Fig. 3 Period B), and in marine air with minor terrestrial  
12 influence (Fig 3. Period F). (b) average absolute number concentrations of CCN (hourly)  
13 during the same periods. Error bars are one standard error of the mean

14 Figure 6. Time series from BB2 including wind direction and rainfall, CN<sub>3</sub> (particle number  
15  $> 3$  nm), CO (carbon monoxide), BC (black carbon), acetonitrile and ratio of acetonitrile to  
16 CO, O<sub>3</sub> and HFC-134a. Events corresponding to Periods A–D are discussed in the text.

17 Figure 7. Emission ratios (ER) of several trace gas and aerosol species to CO during Period A  
18 in BB2

19